Biomedicine & Pharmacotherapy 177 (2024) 117066

Contents lists available at ScienceDirect

Biomedicine & Pharmacotherapy

journal homepage: www.elsevier.com/locate/biopha

Immunomodulatory imide drugs inhibit human detrusor smooth muscle contraction and growth of human detrusor smooth muscle cells, and exhibit vaso-regulatory functions

Alexander Tamalunas [a,d,*,1], Amin Wendt [a], Florian Springer [a], Victor Vigodski [a], Moritz Trieb [a], Nikolaus Eitelberger [a], Henrik Poth [a], Anna Ciotkowska [a], Beata Rutz [a], Sheng Hu [a], Heiko Schulz [b], Stephan Ledderose [b], Nina Rogenhofer [c], Thomas Kolben [c], Elfriede Nössner [d], Christian G. Stief [a], Martin Hennenberg [a]

[a] Department of Urology, University Hospital Munich, LMU Munich, Munich, Germany
[b] Department of Pathology, University Hospital Munich, LMU Munich, Munich, Germany
[c] Department of Obstetrics and Gynecology, University Hospital Munich, LMU Munich, Munich, Germany
[d] Immunoanalytics Research Group Tissue Control of Immunocytes, Helmholtz Center Munich, Munich, Germany

ARTICLE INFO

Keywords:
Lower urinary tract symptoms (LUTS)
overactive bladder (OAB)
bladder smooth muscle contraction
bladder smooth muscle cell proliferation
thalidomide
lenalidomide
pomalidomide

ABSTRACT

Background: The immunomodulatory imide drugs (IMiDs) thalidomide, lenalidomide and pomalidomide may exhibit therapeutic efficacy in the prostate. In lower urinary tract symptoms (LUTS), voiding and storage disorders may arise from benign prostate hyperplasia, or overactive bladder. While current therapeutic options target smooth muscle contraction or cell proliferation, side effects are mostly cardiovascular. Therefore, we investigated effects of IMiDs on human detrusor and porcine artery smooth muscle contraction, and growth-related functions in detrusor smooth muscle cells (HBdSMC).

Methods: Cell viability was assessed by CCK8, and apoptosis and cell death by flow cytometry in cultured HBdSMC. Contractions of human detrusor tissues and porcine interlobar and coronary arteries were induced by contractile agonists, or electric field stimulation (EFS) in the presence or absence of an IMID using an organ bath. Proliferation was assessed by EdU assay and colony formation, cytoskeletal organization by phalloidin staining,

Results: Depending on tissue type, IMiDs inhibited cholinergic contractions with varying degree, up to 50 %, while non-cholinergic contractions were inhibited up to 80 % and 60 % for U46619 and endothelin-1, respectively, and EFS-induced contractions up to 75 %. IMiDs reduced viable HBdSM cells in a time-dependent manner. Correspondingly, proliferation was reduced, without showing pro-apoptotic effects. In parallel, IMiDs induced cytoskeletal disorganization.

Conclusions: IMiDs exhibit regulatory functions in various smooth muscle-rich tissues, and of cell proliferation in the lower urinary tract. This points to a novel drug class effect for IMiDs, in which the molecular mechanisms of action of IMiDs merit further consideration for the application in LUTS.

Abbreviations: 5-AR, 5α-reductase; 5-ARI, 5α-reductase inhibitor; 7-AAD, 7-aminoactinomycin D; ANOVA, analysis of variance; APC, allophycocyanin; α-SMA, α-smooth muscle actin; AUC, area under curve; BFGF, basic fibroblast growth factor; BOO, bladder outlet obstruction; BPH, benign prostatic hyperplasia; CCK-8, cell counting kit 8; DAPI, 4',6-diamidino-2-phenylindole; DHT, dihydrotestosterone; DMSO, dimethylsulfoxide; EAU, European Association of Urology; EdU, 5-ethynyl-2'-deoxyuridine; EFS, electric field stimulation; ENL, erythema nodosum leprosum; FCS, fetal calf serum; FDA, food and drug administration; FITC, fluorescein isothiocyanate; HBdSMC, human bladder detrusor smooth muscle cells; IMiDs, immunomodulatory imide drugs; KCl, potassium chloride; LUTS, lower urinary tract symptoms; OAB, overactive bladder; OD, optical density; PBS, phosphate-buffered saline; PDE5, phosphodiesterase-5; SD, standard deviation; SRB, sulforhodamine B; STEPS, System for Thalidomide Education and Prescribing Safety; TAMRA, tetramethylrhodamine; TCA, trichloroacetic acid; TGF-β, transforming growth factor β; TXA2, thromboxane A2; VEGF, vascular endothelial growth factor.

* Correspondence to: Department of Urology, University Hospital, LMU Munich, Munich, Germany.
E-mail address: alexander.tamalunas@med.uni-muenchen.de (A. Tamalunas).
[1] ORCID ID: 0000–0002-4659–2262

https://doi.org/10.1016/j.biopha.2024.117066

Available online 8 July 2024

1. Introduction

In lower urinary tract symptoms (LUTS), voiding and storage disorders may arise from separate pathologies i.e., overactive bladder (OAB), or benign prostate hyperplasia (BPH), respectively. While patients may suffer from either BPH or OAB, updated European Association of Urology (EAU) guidelines consider the rising number of patients suffering from both at once, so called mixed LUTS [1]. Spontaneous contractions of the detrusor smooth muscle may cause storage symptoms, referred to as OAB [2]. Urethral obstruction leading to voiding symptoms is most commonly attributed to BPH, where hyperplastic growth and increased smooth muscle tone in the prostate may lead to bladder outlet obstruction (BOO) [1,3]. While there is evidence that OAB-related symptoms may present because of BOO, both are separate processes, which may occur simultaneously in patients, so-called "mixed LUTS" [1,4]. In 2018, an estimated 2.7 billion patients suffered from storage symptoms and 1.1 billion patients suffered from voiding symptoms [5]. In both storage and voiding symptoms, the exaggerated smooth muscle tone is an important target of pharmacotherapy [1,3].

Standard-of-care medical treatment for storage symptoms in OAB includes muscarinic receptor antagonists for relief of spontaneous bladder contractions [1,2]. However, efficacy is limited and only slightly superior to placebo [6]. To cite specific pertinent observations, the number of incontinence episodes was reduced by 68 % or 77 % by 7.5 mg or 15 mg darifenacin, and by 54 % and 58 % in corresponding control groups. In the same analysis, the percentage of patients attaining a normal voiding frequency (<8 voids/day) amounted to 34 % and 35 % with 7.5 mg or 15 mg darifenacin, and to 27 % and 28 % in corresponding control groups [6]. Side effects may be bothersome, or often treatment-limiting, and include dry mouth, obstipation, tachycardia, and cognitive impairment, leading to high discontinuation rates [7,8]. The more recent introduction of mirabegron, a β_3-adrenoceptor agonist, for treatment of storage symptoms reflects the need for new substance classes for LUTS pharmacotherapy [1,9]. Recently, clinical trials have increasingly focused on combination therapies, reflecting on the substantial number of patients suffering from mixed LUTS [1,3]. EAU guidelines recommend combining α_1-blockers with muscarinic receptor antagonists for patients suffering from persisting storage symptoms while undergoing α_1-blocker monotherapy [1]. Thus, two main mechanisms of action are targeted at once i.e., α_1-blockade in the prostate and inhibition of muscarinic receptors in the bladder. Side effects of α_1-blockers are mostly cardiovascular, and include hypotension, dizziness, and a tendency to fall. However, adverse events of both drug classes are seen with combined treatment using α_1-blockers and antimuscarinics, and are disproportionately more common and bothersome [10]. Respective discontinuation rates of up to 90 % due to treatment failure or therapy-limiting side effects highlight the limitations of current pharmacotherapy and the need for novel agents with improved efficacy [7,11].

Recent observations showed that immunomodulatory imide drugs (IMiDs) thalidomide, lenalidomide, and pomalidomide inhibited prostate smooth muscle contraction, and may exert regulative action of prostatic hyperplastic growth [12,13]. Potential for new LUTS medications lies in drugs simultaneously inhibiting prostate and bladder smooth muscle contraction, and cell proliferation, without cardiovascular side effects by using a single compound. Lenalidomide and pomalidomide are both structurally similar derivatives of thalidomide, known for causing birth defects following its use as an anti-emetic in pregnant women in the 1960s [14]. Meanwhile, lenalidomide is an established and highly effective treatment in multiple myeloma [15]. Furthermore, oral administration of thalidomide and lenalidomide is safe for treating erythema nodosum leprosum (ENL) [16–18], while recent studies have focused on its antiangiogenic properties in gastrointestinal bleeding [19]. Thus, the translational value of thalidomide and its analogues is high – in particular, in elderly male patients, where the risk of teratogenicity does not apply. Considering recent promising results from the prostate and the obvious translational potential, we here investigated the effects of IMiDs on smooth muscle contraction of human bladder detrusor tissues, and of porcine renal interlobar and coronary arteries, and on proliferation, viability, apoptosis and cell death, and actin organization of human bladder smooth muscle cells.

2. Materials and methods

2.1. Tissues

2.1.1. Human bladder tissues

Human detrusor tissues were obtained from n=174 patients who underwent radical cystectomy for bladder cancer at our tertiary referral center. Detrusor tissues were obtained from both male and female patients [20,21]. Our research was carried out in accordance with the Declaration of Helsinki of the World Medical Association and has been approved by the ethics committee of Ludwig Maximilians University, Munich, Germany. Informed consent was obtained from all patients. While individual patient characteristics may be similar to our previous publications, with a median age of 70 years [20,21], all samples and data were collected and analyzed anonymously. After collection, the bladder specimen was transported in tissue protective custodiol® solution (cat. no. 2328472, Franz Köhler Chemie, Bensheim, Germany). For macroscopic examination and sampling, the bladder was opened by cutting from the bladder outlet to the bladder dome. Subsequently, the intravesical surface and bladder wall were checked macroscopically for tumor infiltration. Tissues were taken from the inner lateral bladder wall if tumor burden in the bladder wall allowed sampling. Urothelial layers were removed from samples. Organ bath studies were performed immediately after sampling.

2.1.2. Porcine arteries

Kidneys (n=92) and hearts (n=80) were obtained from pigs sacrificed for meat production at an age of up to 12 months. Pigs were either females or castrated males. Organs were transported to a nearby butcher shop (Metzgerei Brehm, Planegg, Germany), directly following slaughter during the night (transport and temporary storage at 4 °C). In the morning, organs were transferred to the laboratory. Preparation of interlobar arteries from kidneys, and of middle sections of left anterior descending arteries was started immediately. Adipose and connective tissues were removed from dissected arteries, and vessels were cut into rings, which were stored in custodiol® solution at 4 °C until being used. Arteries were not denuded prior to experiments, which were started within three hours after vessel preparation. Diameters of renal interlobar arteries ranged between 3 and 4 mm, and around 5 mm for coronary arteries.

2.1.3. Tension measurements

Detrusor tissues were prepared into strips (6 ×3×3 mm), while arteries were cut into rings (3–4 mm in length) and mounted in 10 ml aerated (95 % O_2 and 5 % CO_2) tissue baths (Danish Myotechnology, Aahus, Denmark) with four chambers, each containing Krebs-Henseleit solution (37 °C, pH 7.4) with following composition: 118 mM NaCl (cat. no. 3957.2), 4.7 mM KCl (cat. no. 6781.2), 2.55 mM $CaCl_2$ (cat. no. T885.2), 1.2 mM KH_2PO_4 (cat. no. 3904.2), 1.2 mM $MgSO_4$ (cat. no. P027.1), 25 mM $NaHCO_3$ (cat. no. 6885.2), and 7.5 mM glucose (cat. no. X997.3), all purchased from Carl Roth GmbH & Co. KG, Karlsruhe, Germany. Tissue strips were stretched to 4.9 mN for human detrusor tissues, and to 10 mN and 20 mN for porcine renal and coronary arteries, respectively, and left to equilibrate for 45 minutes. In the initial phase of the equilibration period, spontaneous decreases in tone are common and warrant readjusting. Therefore, tensions were adjusted three times during the equilibration period, until a stable resting tone of the respective tension was attained. After the equilibration period, maximum contraction was induced by elevation of potassium concentration to 80 mM, by addition of a 2 M potassium chloride (KCl) solution

to each organ bath chamber (10 ml) in a hyperosmolar manner. Once a plateau or maximum contraction was obviously obtained, chambers were washed three times with Krebs-Henseleit solution for a total of 30 min. Subsequently thalidomide, lenalidomide, or pomalidomide, amounting to final concentrations of 1–1000 μM, 0.2–20 μM, and 0.05–5 μM, respectively, or equivalent amounts of DMSO for controls were added. Cumulative concentration response curves were recorded for porcine renal interlobar arteries with noradrenaline (cat. no. 74480, Sigma-Aldrich, St. Louis, Missouri, USA), phenylephrine (cat. no. 6126, Sigma-Aldrich, St. Louis, Missouri, USA), methoxamine (cat. no. M6524, Sigma-Aldrich, St. Louis, Missouri, USA), endothelin-1 (cat. no. ALX-155–001-P001, Enzo Life Sciences GmbH, Lörrach, Germany) and U46619 (cat. no. 1932, Tocris Bioscience, Bristol, UK), and for human detrusor specimens and porcine coronary arteries with methacholine (cat. no. PHR1943, Sigma-Aldrich, St. Louis, Missouri, USA), carbachol (cat. no. C5259, Sigma-Aldrich, St. Louis, Missouri, USA), endothelin-1 and U46619. Frequency response curves were induced by electric field stimulation (EFS), which stimulates neuronal action potentials, leading to contraction by release of endogenous neurotransmitters [22]. Curves were constructed 30 min after addition of the test compounds or corresponding solvent. Stock solutions of inhibitors were prepared, so that 100 μl of stock solutions or of corresponding solvent were added to organ bath chambers. Each chamber contained 10 ml Krebs-Henseleit solution, resulting in final concentrations of 0.99 % for DMSO. For each test compound, separate control groups were performed. Effects of test compounds and corresponding controls were examined in experiments using samples from the same specimen in each experiment. Within the same experiment, samples from one tissue were allocated to a control, and test compound group, so that both groups in each series were paired and had identical group sizes. Moreover, application of solvent (two chambers), and test compound (two chambers) to chambers was changed for each experiment. All values of one independent experiment were determined in duplicate, wherever this was possible. Thus, two chambers were run for controls, and two other chambers for the test compound in each experiment if the size of sampled tissues allowed this. In experiments, where only two or three chambers could be examined due to limited amount of tissue, or due to discontinuation of single channels for technical reasons, at least one tissue was examined with the test compound and another tissue from the same specimen with corresponding solvent. For each sample only one curve was recorded (original traces shown in supplementary fig. 1–16). Contractions were expressed as percentage of KCl-induced contractions for calculation of agonist-induced contractions. This accounts for the different smooth muscle content and any other heterogeneity between specimen samples, and for small differences in tissue size. For vessel rings, reference to KCl allows to visualize changes in receptor responsiveness, while correlations between force generation and absolute tissue length, diameter, or weight are poor or even completely lacking in organ bath experiments [23]. In addition to the construction of concentration response curves, EC_{50} values for contractile agonists, and Ef_{50} values for frequency-induced contractions (f), and E_{max} values were calculated by curve fitting. Curve fitting was performed separately for each single experiment, using GraphPad Prism 9.3.0 (GraphPad Software Inc., San Diego, CA, USA), and values were analyzed as described below. Frequency response curves and concentration response curves were fitted without predefined constraints for bottom, top, or EC_{50} values, by ordinary fit, without weighting, and without choosing automatic outlier elimination by non-linear regression. Resulting values were checked for plausibility and settings were adapted if error messages occurred, as recommended in the "GraphPad Curve Fitting Guide". In some cases, the fitted EC_{50} values may have underestimated the actual values, due to lack of experimental points at lowest concentrations defining an accurate lower limit baseline for fitting.

2.2. Cell culture

Human bladder detrusor smooth muscle cells (HBdSMC) isolated from human bladder tissue were obtained from ScienCell Research Laboratories (Cat. No. 4310, lot no. 5828, Carlsbad, CA, USA). According to the manufacturer, HBdSMC are primary cells isolated from human bladder tissue, positive for smooth muscle α-actin and fibronectin, negative for CD 90 and desmin. Potential contaminations by human immunodeficiency virus (HIV-1), hepatitis B virus (HBV), hepatitis C virus (HCV), mycoplasma, and bacteria or fungi has been tested and ruled out. HBdSMC were cultured in smooth muscle cell medium (SMCM medium; cat. no. 1101; ScienCell, Carlsbad, California, USA) containing 2 % fetal calf serum (FCS; cat. no. A5256801, Gibco Fisher Scientific GmbH, Schwerte, Germany) together with smooth muscle cell growth supplement and 1 % penicillin/streptomycin (cat. no. 10378–016; Gibco Fisher Scientific GmbH, Schwerte, Germany) at 37 °C with 5 % CO_2, according to the manufacturer's recommendations. Before addition of either IMiD, or DMSO (cat. no. 3176, Tocris Biosciences, Bristol, UK) for controls, the medium was changed to FCS-free medium. Change of medium was performed every day until cells were confluent. After cell counting and determination of proportionate volume required for further experiments, cells were transferred to culture vessels of respective experiments. For cell culture experiments, three working solutions of each IMiD were prepared. The final concentration for cell culture experiments was 10, 30, and 100 μM for thalidomide, 5, 10, and 30 μM for lenalidomide, and 2.5, 5, and 10 μM for pomalidomide.

2.2.1. Cell proliferation assay

HBdSM cells were plated with a density of 30,000/well on a 12-well chambered coverslip (cat. no. 81201, Ibidi, Munich, Germany). Cells were grown until a confluence of 60–80 % was reached. After this growth period, the medium was changed to a 10 mM 5-ethynyl-2'-deoxyuridine (EdU) solution in FCS-free medium containing inhibitors or solvent, and cells were treated with either thalidomide, lenalidomide, or pomalidomide at the pre-specified concentrations, and equivalent amounts of dimethylsulfoxide (DMSO) for controls and grown for a subsequent period of 24 hours. Following the exposure period, cells were fixed with 3.7 % formaldehyde (cat. no. P087.5, Carl Roth GmbH & Co. KG, Karlsruhe, Germany). EdU incorporation was determined using the "EdU-Click 555" cell proliferation assay (cat. no. BCK-EdU555IM100, Baseclick, Tutzing, Germany) according to the manufacturer`s instructions. Incorporation of EdU into DNA is assessed by detection through fluorescing 5-carboxytetramethylrhodamine (5-TAMRA), while counterstaining of all nuclei was performed with DAPI (4',6-diamidino-2-phenylindole; cat. no. D1306, Invitrogen by Fisher Scientific GmbH, Schwerte, Germany). Cells were then analyzed by fluorescence microscopy (excitation: 546 nm; emission: 479 nm), and 25 representative images of each well were taken. Blinding was used as randomization method. Each experiment was repeated five times. Thereby, each whole coverslip represents one individual experiment. Subsequently, the number of proliferating cells (i.e., EdU stained cells) was calculated in the microscopic field using ImageJ cell counter (U.S. National Institutes of Health, Bethesda, Maryland, USA). Cells are calculated individually for each experiment as a proliferation ratio (EdU stained cells divided by DAPI stained nuclei).

2.2.2. Plate colony assay

The ability of adherent cells to organize into colonies (> 50 cells) after exposure to a specific agent can be quantified using a plate colony assay [24,25]. HBdSM cells were seeded in Falcon 6-well tissue culture plates (cat. no. 10110151, Fisher Scientific GmbH, Schwerte, Germany) at 100 cells/well and incubated at 37 °C for 168 hours. After the initial growth period, cells were either exposed to thalidomide, lenalidomide, and pomalidomide, or equal amounts of solvent (DMSO) for controls and incubated for an additional period of 168 hours. Cells were washed

twice with phosphate-buffered saline (PBS; cat. no. 9143.1, Carl Roth GmbH & Co. KG, Karlsruhe, Germany) and fixed by 2 ml 10 % trichloroacetic acid (TCA; cat. no. T0699, Sigma-Aldrich, St. Louis, Missouri, USA) at 4 °C overnight. After that, all plates were washed five times with cold water, and stained with 0.4 % sulforhodamine B (SRB; cat. no. 341738, Sigma-Aldrich, St. Louis, Missouri, USA) solution (diluted in 1 % acetic acid) at room temperature for 30 minutes. Before analysis, all plates were labeled and washed by 1 % acetic acid (cat. no. 6755.1, Carl Roth GmbH & Co. KG, Karlsruhe, Germany) five times. Finally, colonies were assessed under white light, with the number of cell colonies being calculated individually for each experiment using ImageJ cell counter (U. S. National Institutes of Health, Bethesda, Maryland, USA).

2.2.3. Cell viability assay

The effects of thalidomide, lenalidomide and pomalidomide on cell viability were assessed using the Cell Counting Kit-8 (CCK-8) (cat. no. 96992–500 T, Sigma-Aldrich, St. Louis, Missouri, USA). Cells were grown in 96-well plates (20,000 cells/well) for 24 h, before either thalidomide, lenalidomide or pomalidomide at pre-specified concentrations, and equivalent amounts of DMSO for controls were added. For each concentration and time, series of n=5 independent experiments were performed. Subsequently, cells were grown for a period of 24, 48, and 72 hours with separate controls for each substance. After the respective growth periods, 10 µl of 2-(2-methoxy-4-nitrophenyl)-3-(4-nitrophenyl)-5-(2,4-disulfophenyl)-2 H-tetrazolium mono-sodium salt (WST-8) from CCK-8 were added, and absorbance (optical density, OD) in each well was measured at 450 nm after incubation for 120 minutes at 37 °C.

2.2.4. Flow cytometry analysis for apoptosis and cell death

A flow cytometry-based annexin V allophycocyanin (APC) and 7-aminoactinomycin D (7-AAD) apoptosis detection kit (BD Biosciences, Franklin Lakes, NJ, USA) was used to detect cells in apoptosis (annexin V-positive, 7-AAD-negative) and dead cells (annexin V-positive, 7-AAD-positive). HBdSM cells were seeded in Falcon 6-well tissue culture plates (cat. no. 10110151, Fisher Scientific GmbH, Schwerte, Germany) at 250,000 cells/well and incubated at 37 °C for 24 hours. After addition of either thalidomide, lenalidomide or pomalidomide at pre-specified concentrations, and equivalent amounts of DMSO for controls, cells were incubated for another 72 hours. Subsequently, cells were washed with phosphate-buffered saline (PBS) and resuspended in annexin V binding buffer (cat. no. 556454, BD Biosciences, Franklin Lakes, NJ, USA), followed by addition of 5 µl Allophycocyanin (APC)-coupled annexin V (cat. no. 550475, BD Biosciences, Franklin Lakes, NJ, USA) and 5 µl 7-AAD reagent (cat. no. 559925, BD Biosciences, Franklin Lakes, NJ, USA) to each sample. After incubation in the dark for 15 minutes at room temperature, 400 µl binding buffer were added to each sample before analysis by flow cytometry. Fluorescence activated cell sorting (FACS) was performed using BD FACSCalibur™ Cytometer (BD Biosciences, Franklin Lakes, NJ, USA) and Flo Jo Software v8.8.7 (FlowJo LLC, Ashland, Oregon) for final analysis. Gating parameters were set utilizing fluorescence-minus-one (FMO) controls, which involves the use of all the antibodies in the panel minus the one for which the appropriate gate must be determined, including controls for cells untreated and unstained, treated and unstained, and untreated and stained [26]. The first step was to establish appropriate forward scatter (FSC) and side scatter (SSC) gates to identify the desired cells and exclude cell debris and cell aggerates by separating HBdSM cells from cell fragments that were located near the ordinate due to their smaller area in the forward scatter (FSC-A) to side scatter (SSC-A) representation. Next, the cells were displayed using FSC-A (area) against FSC-H (height) to separate the singlets. As FSC is a measure of cell volume and clumped cells have a relatively large surface area despite their low height, they could be excluded according to this criterion. This was followed by determination of the background from the other fluorochromes in the detector that is being used to measure the target fluorochrome, using a 635-nm red laser for excitation of APC Annexin V, and a 488-nm blue laser for excitation of "ready-to-use nucleic acid dye" 7-AAD. Based on these settings, 10,000 events were analyzed for each sample using ModFit LT™ software (Verity Software House, Torpsham, ME, USA).

2.2.5. Phalloidin staining

For fluorescence staining with phalloidin, cells were seeded at a density of 30,000/well and grown on 16-well chambered coverslip. After 24 hours, cells were treated with either thalidomide, lenalidomide or pomalidomide at pre-specified concentrations, and equivalent amounts of DMSO for controls and grown for a subsequent period of 24 hours. Staining was performed using 100 µM fluorescein isothiocyanate (FITC)-labeled phalloidin (cat. no. P5282, Sigma-Aldrich, St. Louis, Missouri, USA), according to the manufacturer's instruction, while counterstaining of all nuclei was performed with DAPI (4',6-diamidino-2-phenylindole). Labeled cells were analyzed using a laser scanning microscope (Leica SP8 AOBS WLL, Wetzlar, Germany).

2.3. Data and statistical analysis

Data in frequency and concentration response curves are presented in graphs as means ± standard deviation (SD). E_{max}, pEC_{50}, Ef_{50}, IC_{50} values and data from cell culture are presented as single values from each independent experiment, together with means in scatter plots, where related samples from one experiment are indicated by corresponding symbols. Effect sizes become obvious from frequency and concentration response curves, and from scatter plots, and are summarized in a simplified manner in the text. Details are given in Table 1 and Table 2, as an overview for comparison between the effects of inhibitors and control tissues, while only statistically significant E_{max}, and pEC_{50} values for contractile agonists, and frequencies (f) inducing 50 % of the maximum EFS-induced contraction (Ef_{50}) are stated in the text. Statistical analyses were performed using GraphPad Prism Version 9.3.0 (GraphPad Software Inc., San Diego, CA, USA). Comparison of whole frequency/concentration response curves was performed by two-way analysis of variance (ANOVA). Areas under the curves (AUC) were calculated for concentration and frequency response curves in each single experiment, in the presence of inhibitors (i.e., pomalidomide, lenalidomide, and thalidomide) and in controls (DMSO) of the same series, which are given with 95 % CI for all frequencies, agonist concentrations, and experiments in each series, with the corresponding p values in the upper left-hand corner of the diagrams in each figure. AUC represent the total area under the curve, expressed as percentage to high-molar KCl-induced contractions. Values for AUC are dimensionless and therefore given as arbitrary units (a.u.). E_{max}, pEC_{50}, and Ef_{50} values were calculated for each single experiment by curve fitting and are given including corresponding absolute mean difference (MD). Curve fitting was performed separately for each single experiment, using GraphPad Prism 9.3.0 (GraphPad Software, Boston, MA, USA), and values were analyzed as previously described [27,28]: curves were fitted without predefined constraints for bottom, top or EC_{50} values, by ordinary fit, without weighting, and without choosing automatic outlier elimination by non-linear regression. As recommended in the "GraphPad Curve Fitting Guide" (GraphPad Software Inc., San Diego, CA, USA), resulting values were checked for plausibility, and the program labels values with error messages ("not converged" or "ambiguous") if it considers values as non-plausible or if curve fitting is not possible. Specifically, uphill parts of curves were used for curve fitting, as curves could not be converged if downhill portions were included, from concentration-response curves with cholinergic agonists. E_{max}, pEC_{50}, and Ef_{50} values were calculated and compared by a paired Student's t-test. The present study and analyses show an exploratory design and were not designed to test a pre-specified statistical null hypothesis, for previously described reasons [29]. Accordingly, p values reported here

Table 1
Detailed results for contractions of human detrusor tissues, and vasoconstriction of porcine coronary, and renal interlobar arteries.

(A) AUC						
Pomalidomide	**bladder control**	**Pomalidomide**	**coronary artery control**	**Pomalidomide**	**renal artery control**	**Pomalidomide**
MCH	881 [738–1024]	572 [477–667]	1495 [916–2075]	659 [482–836]		
CCH	806 [643–969]	596 [505–687]	1463 [660–2265]	580 [426–733]		
U46619	148 [113–183]	85 [66–105]	1312 [799–1825]	749 [432–1066]	1297 [955–1639]	635 [474–796]
ET-1	191 [152–229]	124 [105–142]	1179 [540–1819]	596 [163–1029]	1013 [458–1568]	382 [202–562]
EFS	444 [286–602]	288 [197–379]	61 [0–158]	18 [0–57]	273 [114–431]	173 [97–249]
NA					4822 [3608–6036]	2366 [1217–3516]
PE					1631 [1212–2050]	600 [438–762]
MXE					1011 [694–1329]	495 [403–586]
Lenalidomide	**bladder control**	**Lenalidomide**	**coronary artery control**	**Lenalidomide**	**renal artery control**	**Lenalidomide**
MCH	1063 [824–1302]	603 [469–737]	1975 [1601–2348]	1104 [808–1400]		
CCH	845 [755–936]	551 [494–607]	1276 [686–1867]	566 [410–721]		
U46619	168 [145–191]	96 [69–123]	877 [498–1256]	460 [144–775]	1037 [560–1514]	460 [220–700]
ET-1	206 [173–238]	101 [61–140]	127 [576–2067]	677 [269–1085]	1553 [689–2417]	824 [414–1233]
EFS	475 [419–531]	493 [416–569]	118 [85–151]	62 [35–89]	258 [153–362]	93 [14–172]
NA					2692 [731–4652]	1362 [572–2152]
PE					1237 [1001–1474]	590 [493–687]
MXE					856 [613–1105]	536 [355–717]
Thalidomide	**bladder control**	**Thalidomide**	**coronary artery control**	**Thalidomide**	**renal artery control**	**Thalidomide**
MCH	967 [751–1186]	705 [637–772]	1090 [434–1747]	520 [192–848]		
CCH	700 [597–803]	554 [440–668]	907 [702–1113]	808 [542–1075]		
U46619	247 [165–329]	132 [81–184]	919 [763–1074]	136 [45–215]	1269 [556–1982]	1164 [712–1615]
ET-1	198 [131–265]	121 [90–152]	1133 [260–2006]	643 [202–1084]	931 [236–1664]	427 [80–774]
EFS	552 [456–648]	475 [408–542]	77 [0–173]	22 [0–84]	261 [45–477]	143 [19–267]
NA					2878 [1600–4156]	2553 [1041–4066]
PE					1333 [1146–1519]	1003 [799–1208]
MXE					632 [439–826]	486 [315–658]

(B) E_{max}						
Pomalidomide	**bladder control**	**Pomalidomide**	**coronary artery control**	**Pomalidomide**	**renal artery control**	**Pomalidomide**
MCH	127 [98–155]	80 [62–97]	231 [79–384]	87 [41–134]		
CCH	104 [59–149]	86 [64–108]	227 [88–366]	80 [30–129]		
U46619	33 [18–48]	18 [12–25]	233 [27–439]	133 [4–261]	235 [92–377]	105 [50–160]
ET-1	75 [54–97]	56 [46–66]	434 [90–778]	228 [-3–458]	406 [122–690]	159 [64–253]
EFS	195 [127–264]	114 [88–141]	44 [4–121]	19 [4–35]	148 [65–231]	83 [35–131]
NA					1066 [636–1497]	442 [159–726]
PE					376 [242–509]	127 [54–201]
MXE					231 [101–361]	117 [86–148]
Lenalidomide	**bladder control**	**Lenalidomide**	**coronary artery control**	**Lenalidomide**	**renal artery control**	**Lenalidomide**
MCH	141 [82–200]	84 [47–121]	279 [150–408]	140 [82–198]		
CCH	116 [81–151]	76 [60–92]	216 [21–411]	80 [29–131]		
U46619	33 [26–41]	20 [12–28]	140 [13–267]	89 [-14–191]	218 [34–401]	83 [-2–167]
ET-1	71 [54–89]	42 [26–57]	410 [71–749]	229 [44–413]	465 [109–821]	262 [35–489]
EFS	144 [120–167]	146 [120–173]	46 [29–63]	23 [13–32]	125 [48–202]	59 [-9–128]
NA					532 [6–1058]	331 [-42–705]
PE					292 [190–393]	141 [108–174]
MXE					190 [76–303]	123 [40–207]
Thalidomide	**bladder control**	**Thalidomide**	**coronary artery control**	**Thalidomide**	**renal artery control**	**Thalidomide**
MCH	135 [69–200]	101 [90–113]	175 [-4–353]	82 [-7–170]		
CCH	101 [76–126]	80 [61–99]	184 [125–244]	165 [82–247]		
U46619	60 [29–92]	31 [9–53]	161 [122–200]	40 [25–56]	224 [42–408]	219 [54–383]
ET-1	77 [34–120]	48 [27–70]	355 [-4–704]	213 [-6–431]	320 [19–621]	187 [1–373]
EFS	152 [100–204]	152 [128–175]	31 [0–62]	18 [0–36]	166 [32–301]	69 [2–136]
NA					680 [62–1298]	648 [16–1296]
PE					303 [233–372]	214 [129–300]
MXE					160 [101–218]	133 [66–201]

(C) pEC_{50}/Ef_{50}						
Pomalidomide	**bladder control**	**Pomalidomide**	**coronary artery control**	**Pomalidomide**	**renal artery control**	**Pomalidomide**
MCH	6.6 [5.9–7.2]	6.9 [6.3–7.4]	6.6 [6.2–6.9]	7.1 [6.8–7.4]		
CCH	7.2 [6.8–7.5]	6.7 [6.1–7.3]	6.5 [6.1–6.9]	6.8 [6.4–7.1]		
U46619	5.9 [5.0–6.7]	6.1 [5.1–7.1]	6.4 [6.1–6.8]	6.6 [6.2–7.0]	6.6 [5.9–7.3]	6.7 [6.2–7.3]
ET-1	6.5 [6.2–6.8]	6.2 [5.9–6.5]	6.3 [5.6–7.1]	6.1 [5.3–6.9]	6.7 [6.0–7.4]	6.2 [5.6–8.8]
EFS	9.2 [6.5–11.8]	8.0 [4.4–11.6]	7.2 [1.0–13.6]	10.3 [3.6–16.9]	13.2 [7.9–18.5]	9.5 [4.9–14.2]
NA					6.4 [6.1–6.8]	6.2 [6.0–6.3]
PE					6.4 [5.8–7.1]	6.5 [6.3–6.7]
MXE					6.3 [5.8–6.7]	6.2 [5.7–6.7]

(*continued on next page*)

Table 1 (*continued*)

(C) pEC_{50}/Ef_{50} Pomalidomide	bladder control	Pomalidomide	coronary artery control	Pomalidomide	renal artery control	Pomalidomide
Lenalidomide	**bladder control**	**Lenalidomide**	**coronary artery control**	**Lenalidomide**	**renal artery control**	**Lenalidomide**
MCH	7.1 [6.4–7.7]	7.1 [6.2–8.0]	6.7 [6.5–6.9]	6.6 [6.4–6.8]		
CCH	7.1 [6.8–7.3]	6.9 [6.6–7.2]	5.9 [4.4–7.5]	6.6 [6.0–7.3]		
U46619	6.6 [6.1–7.0]	5.9 [5.0–6.8]	7.0 [6.5–7.5]	6.6 [6.2–7.0]	6.7 [6.3–7.1]	6.8 [6.5–7.1]
ET-1	6.7 [6.3–7.2]	6.2 [5.7–6.8]	6.6 [5.9–7.4]	6.7 [6.2–7.1]	6.7 [6.4–6.9]	6.7 [6.6–6.9]
EFS	3.9 [3.6–4.2]	4.4 [2.6–6.2]	12.7 [7.0–18.4]	10.5 [4.2–16.7]	9.7 [5.7–13.7]	12.9 [7.7–18.2]
NA					6.1 [5.8–6.4]	6.1 [5.9–6.3]
PE					6.2 [6.0–6.3]	6.1 [5.9–6.4]
MXE					6.4 [6.0–6.9]	6.5 [5.6–7.3]
Thalidomide	**bladder control**	**Thalidomide**	**coronary artery control**	**Thalidomide**	**renal artery control**	**Thalidomide**
MCH	6.9 [6.7–7.0]	6.6 [6.3–6.8]	6.8 [6.5–7.2]	6.8 [6.5–7.2]		
CCH	7.1 [6.8–7.3]	6.6 [6.2–7.1]	5.4 [5.0–5.9]	5.3 [4.8–5.8]		
U46619	5.5 [4.5–6.6]	5.6 [4.9–6.2]	6.5 [6.1–6.8]	6.0 [4.8–7.5]	6.6 [6.2–7.1]	6.5 [5.7–7.4]
ET-1	6.6 [6.0–7.2]	6.6 [5.8–7.3]	6.8 [6.2–7.4]	6.8 [6.0–7.6]	6.3 [6.1–6.5]	6.1 [5.6–6.6]
EFS	7.9 [3.0–12.9]	5.2 [3.0–7.3]	9.8 [1.7–17.9]	7.0 [0.2–13.9]	16.0 [15.8–16.2]	11.5 [5.9–17.0]
NA					6.2 [5.4–7.0]	5.9 [5.1–6.8]
PE					6.3 [5.8–6.9]	6.6 [5.9–7.3]
MXE					6.0 [5.1–6.8]	5.8 [5.4–6.2]

Given are results for Area under the curve (A), E_{max} (B), and pEC_{50}/Ef_{50} values (C) for concentration responses following incubation with pomalidomide 5 μM, lenalidomide 20 μM, and thalidomide 100 μM on human detrusor smooth muscle contraction, vasoconstriction of porcine coronary, and renal interlobar arteries. (A) shows the values for AUC with 95 % confidence interval (CI) given as arbitrary units (a.u.), which represent the total area under the curve, (B) shows the values for E_{max} with 95 % confidence interval (CI) given as percentages (%), and (C) shows the values for pEC_{50} for contractile agonists and Ef_{50} for electric field stimulation with 95 % confidence interval (CI) given as arbitrary units (a.u.). Tensions have been calculated and normalized to the contraction induced by high-molar KCl, being assessed before application of inhibitors or equal amounts of DMSO. High-molar KCl-induced contractions are conducted to eliminate heterogeneities due to individual variations or varying smooth muscle content in tissue strips. MCH = methacholine; CCH = carbachol; U46619 = thromboxane A2 analog; ET-1 = endothelin-1; NA = noradrenaline; PE = phenyilephrine; MXE = methoxamine; EFS = electric field stimulation

need to be considered as descriptive, but not as hypothesis-testing. Minimum number of experiments and group sizes for each series were pre-planned as n=5/group, to allow statistical analyses. Data were analyzed, after five or more experiments were performed for a given series. If these initial results were inconclusive i.e., pointed to a possible drug effect but without p values <0.05, series were continued and analyzed again. This procedure was possible due to the explorative character and as long as it is reported in detail [29], and flexible group sizes have been recommended for data being characterized by large variations [30]. However, interim analyses were limited to frequency and concentration response curves and did not include curve fitting, which was intended only after completion of a series. No data or experiments were excluded from analyses.

2.4. Materials, drugs and nomenclature

Thalidomide (N-(2,6-dioxo-3-piperidinyl)phthalimide; cat. no. 0652, Tocris Bioscience, Bristol, UK) binds cereblon and inhibits ubiquitin ligase activity [14,31]. Lenalidomide (3-(4-Amino-1, 3-dihydro-1-oxo-2 H-isoindol-2-yl)-2,6-piperidinedione; cat. no. 6304, Tocris Bioscience, Bristol, UK) is a structural analog of thalidomide. Thalidomide and lenalidomide were stored at −20 °C and stock solutions were freshly prepared before each experiment. Pomalidomide (4-Amino-2-(2,6-dioxo-3-piperidinyl)-1 H-isoindole-1,3(2 H)-dione; cat. no. 6302, Tocris Bioscience, Bristol, UK), like lenalidomide, is a structural derivative of thalidomide. Pomalidomide was stored at 4 °C and stock solutions of were freshly prepared with DMSO before each experiment. Phenylephrine ((R)-3-[-1-hydroxy-2-(methylamino)ethyl] phenol), methoxamine (α-(1-Aminoethyl)-2,5-dimethoxy-benzyl alcohol) and noradrenaline (4-[(1 R)-2-Amino-1-hydroxyethyl]-1, 2-benzenediol) are agonists for α_1-adrenoceptors. Carbachol (carbamoylcholin; (2-Hydroxyethyl)-trimethylammonium-chlorid-carbamat) and methacholine (2-Acetoxypropyl) trimethylam-moniumchlorid, Acetyl-β-methylcholin-chlorid) are muscarinic acetylcholine receptor agonists [32,33]. U46619 ((*Z*)-7-[(1 S,4 R,5 R,6 S)-5-[(*E*,3 S)-3-hydroxyoct-1-enyl]-3-oxabicyclo[2.2.1]heptan-6-yl]hept-5-enoic acid) is an analogue of thromboxane A_2 (TXA_2) and frequently used as an agonist for TXA_2 receptors. Endothelin-1 is a 21-amino acid peptide with high affinity to the endothelin A (ET_A) and B (ET_B) receptors. Aqueous stock solutions of noradrenaline, phenylephrine, and methoxamine were freshly prepared before each experiment. Stock solutions of U46619 were prepared in ethanol and stock solutions of endothelin-1 in water and stored at −80 °C until use.

3. Results

3.1. Contractility measurements

Effect sizes become obvious from frequency and concentration response curves and from scatter plots given in Figs. 1–4. Detailed results are given in Table 1 and for concentration-dependent responses in Table 2. AUC represent an overview for comparison of concentration response and frequency response curves with IMiDs to corresponding curves without IMiDs. Results from post hoc analyses at each concentration in concentration-response curves, using Sidak's multiple comparisons test, can be found in supplementary fig. 17–20. While detailed results for E_{max}, pEC_{50}, and Ef_{50} can be found in Table 1 and 2, only statistically significant E_{max}, and pEC_{50} values for contractile agonists, and Ef_{50} values of the maximum EFS-induced contraction are stated in the following text.

3.1.1. Effects of IMiDs on contraction of human bladder detrusor tissues

3.1.1.1. Cholinergic contractions. Human detrusor smooth muscle contraction was induced by the cholinergic agonists carbachol and methacholine following incubation with pomalidomide (5 μM), lenalidomide (20 μM), and thalidomide (100 μM), or equal amounts of DMSO for controls. For methacholine-induced contractions, AUC in concentration response curves (0.1–1000 μM) was reduced by around one-third for pomalidomide (Fig. 1 A) and thalidomide (Fig. 1 C), and by 40 % for lenalidomide (Fig. 1 B), respectively. E_{max} was reduced only by pomalidomide, amounting to 127 [98−155] % of KCl-induced contractions in

Table 2
Detailed results for concentration-dependent responses on human detrusor smooth muscle contraction.

(A) AUC						
Pomalidomide	**50 µM**		**500 nM**		**50 nM**	
	control	**Pomalidomide**	**control**	**Pomalidomide**	**control**	**Pomalidomide**
MCH	925 [755–1094]	192 [163–220]	1007 [904–1110]	724 [620–827]	902 [787–1018]	745 [638–826]
EFS	447 [350–544]	129 [81–177]	440 [328–552]	328 [258–397]	517 [393–640]	412 [345–479]
Lenalidomide	**200 µM**		**2 µM**		**200 nM**	
	control	**Lenalidomide**	**control**	**Lenalidomide**	**control**	**Lenalidomide**
MCH	894 [714–1074]	277 [218–336]	949 [834–1065]	643 [547–738]	1087 [948–1226]	811 [700–922]
EFS	412 [369–455]	119 [88–151]	437 [374–500]	401 [335–467]	440 [384–496]	424 [334–515]
Thalidomide	**1 mM**		**10 µM**		**1 µM**	
	control	**Thalidomide**	**control**	**Thalidomide**	**control**	**Thalidomide**
MCH	893 [807–979]	272 [227–317]	1095 [895–1295]	844 [689–999]	1126 [962–1290]	954 [819–1090]
EFS	524 [441–608]	149 [127–170]	520 [405–634]	435 [364–507]	566 [460–672]	521 [411–630]
(B) E_{max}						
Pomalidomide	**50 µM**		**500 nM**		**50 nM**	
	control	**Pomalidomide**	**control**	**Pomalidomide**	**control**	**Pomalidomide**
MCH	145 [98–193]	27 [22–33]	148 [125–170]	101 [75–128]	130 [94–165]	106 [74–138]
EFS	182 [132–232]	47 [17–76]	172 [117–227]	123 [100–146]	206 [138–274]	164 [126–201]
Lenalidomide	**200 µM**		**2 µM**		**200 nM**	
	control	**Lenalidomide**	**control**	**Lenalidomide**	**control**	**Lenalidomide**
MCH	130 [75–186]	38 [21–55]	135 [111–159]	96 [66–125]	159 [109–209]	114 [80–149]
EFS	145 [123–166]	38 [24–53]	147 [130–165]	140 [99–181]	165 [134–196]	155 [103–207]
Thalidomide	**1 mM**		**10 µM**		**1 µM**	
	control	**Thalidomide**	**control**	**Thalidomide**	**control**	**Thalidomide**
MCH	143 [126–161]	42 [27–57]	159 [98–221]	121 [69–173]	175 [138–213]	140 [97–182]
EFS	174 [137–211]	50 [45–55]	174 [128–220]	153 [127–180]	193 [144–243]	177 [120–233]
(C) pEC_{50}/Ef_{50}						
Pomalidomide	**50 µM**		**500 nM**		**50 nM**	
	control	**Pomalidomide**	**control**	**Pomalidomide**	**control**	**Pomalidomide**
MCH	6.2 [6.0–6.4]	6.6 [6.2–7.0]	6.5 [6.2–6.7]	6.6 [6.4–6.8]	6.6 [6.4–6.8]	6.6 [6.4–6.8]
EFS	7.4 [5.7–9.2]	6.1 [3.8–8.4]	8.0 [7.7–8.2]	7.8 [7.3–8.2]	7.9 [7.6–8.2]	7.9 [7.8–8.1]
Lenalidomide	**200 µM**		**2 µM**		**200 nM**	
	control	**Lenalidomide**	**control**	**Lenalidomide**	**control**	**Lenalidomide**
MCH	6.5 [6.3–6.7]	6.7 [6.4–7.1]	6.6 [6.4–6.8]	6.4 [6.1–6.7]	6.5 [6.3–6.7]	6.7 [6.3–7.0]
EFS	6.4 [4.0–8.8]	4.9 [2.5–7.4]	5.7 [3.2–8.1]	6.3 [3.7–8.9]	7.2 [5.2–9.1]	6.5 [4.1–9.0]
Thalidomide	**1 mM**		**10 µM**		**1 µM**	
	control	**Thalidomide**	**control**	**Thalidomide**	**control**	**Thalidomide**
MCH	6.1 [5.9–6.4]	6.5 [6.2–6.8]	6.5 [6.3–6.7]	6.5 [6.4–6.6]	6.3 [5.7–6.8]	6.4 [6.2–6.7]
EFS	6.3 [4.0–8.6]	6.3 [3.5–9.2]	6.4 [3.6–9.2]	7.2 [5.1–9.2]	5.7 [3.2–8.2]	5.6 [3.0–8.3]

Given are results for area under the curve (A), E_{max} (B), and pEC_{50}/Ef_{50} values (C) for concentration responses following incubation with pomalidomide at 50 µM, 500 nM, and 50 nM, with lenalidomide at 200 µM, 2 µM, and 200 nM, and with thalidomide at 1 mM, 10 µM, and 1 µM on human detrusor smooth muscle contraction. (A) shows the values for AUC with 95 % confidence interval (CI) given as arbitrary units (a.u.), which represent the total area under the curve, (B) shows the values for E_{max} with 95 % confidence interval (CI) given as percentages (%), and (C) shows the values for pEC_{50} for contractile agonist methacholine, and Ef_{50} for electric field stimulation with 95 % confidence interval (CI) given as arbitrary units (a.u.). Tensions have been calculated and normalized to the contraction induced by high-molar KCl, being assessed before application of inhibitors or equal amounts of DMSO. High-molar KCl-induced contractions are conducted to eliminate heterogeneities due to individual variations or varying smooth muscle content in tissue strips. MCH = methacholine; EFS = electric field stimulation

controls and to 80 [62−97] % of KCl-induced contractions after application of pomalidomide (MD 47 [7−88] %, p=0.0320; Fig. 1A), while remaining unchanged for thalidomide and lenalidomide. EC_{50} values for methacholine were decreased by pomalidomide, reflected by increases of pEC_{50} values from 6.6 [5.9–7.2] in controls to 6.9 [6.3–7.4] after application of pomalidomide (MD 0.3 [0.1–0.5]; p=0.0165; Fig. 1A), while EC_{50} values were increased by thalidomide, reflected by decreases of pEC_{50} values from 6.9 [6.7–7.0] in controls to 6.6 [6.3–6.8] after application of thalidomide (MD 0.3 [0.0–0.6]; p=0.0419; Fig. 1C).

For carbachol-induced contractions, AUC in concentration response curves (0.1–1000 µM) was reduced around one-fourth for pomalidomide (Fig. 1D) and thalidomide (Fig. 1F), and around 40 % for lenalidomide (Fig. 1E). E_{max} was reduced only by lenalidomide, amounting to 116 [81−151] % of KCl-induced contractions in controls and to 76 [60−92] % of KCl-induced contractions after application of lenalidomide (MD 40 [16−65] %, p=0.0105; Fig. 1E), while remaining unchanged for thalidomide and pomalidomide. EC_{50} values for carbachol were increased by thalidomide, reflected by decreases of pEC_{50} values from 7.1 [6.8–7.3] in controls to 6.6 [6.2–7.1] after application of thalidomide (MD 0.4 [0.1–0.8]; p=0.0306; Fig. 1F).

3.1.1.2. Non-cholinergic contractions. All three IMiDs inhibited non-cholinergic contractions induced by U46619 and reduced AUC in concentration response curves (0.01–30 µM) by around 50 % (Fig. 1G to Fig. 1I). E_{max} was reduced by pomalidomide, amounting to 33 [18−48] % of KCl-induced contractions in controls and to 18 [12−25] % of KCl-induced contractions after application of pomalidomide (MD 15 [4−25] %, p=0.0153; Fig. 1G), lenalidomide, amounting to 33 [26−41] % of KCl-induced contractions in controls and to 20 [12−28] % of KCl-induced contractions after application of lenalidomide (MD 13 [4−22] %, p=0.0155; Fig. 1H), and thalidomide, amounting to 60 [29−92] % of KCl-induced contractions in controls and to 31 [9−53] % of KCl-induced contractions after application of thalidomide (MD 29 [13−45] %, p=0.0077; Fig. 1I). EC_{50} values remained unchanged for U46619-induced contractions.

AUC in concentration response curves (0.1–10 µM) for endothelin-1-induced contractions were reduced around 40 % for pomalidomide (Fig. 1J) and thalidomide (Fig. 1L), respectively, and by around 50 % for lenalidomide (Fig. 1 K). E_{max} was reduced by pomalidomide, amounting to 75 [54−97] % of KCl-induced contractions in controls and to 56 [46−66] % of KCl-induced contractions after application of pomalidomide (MD 19 [1−38] %, p=0.0416; Fig. 1J), lenalidomide, amounting to

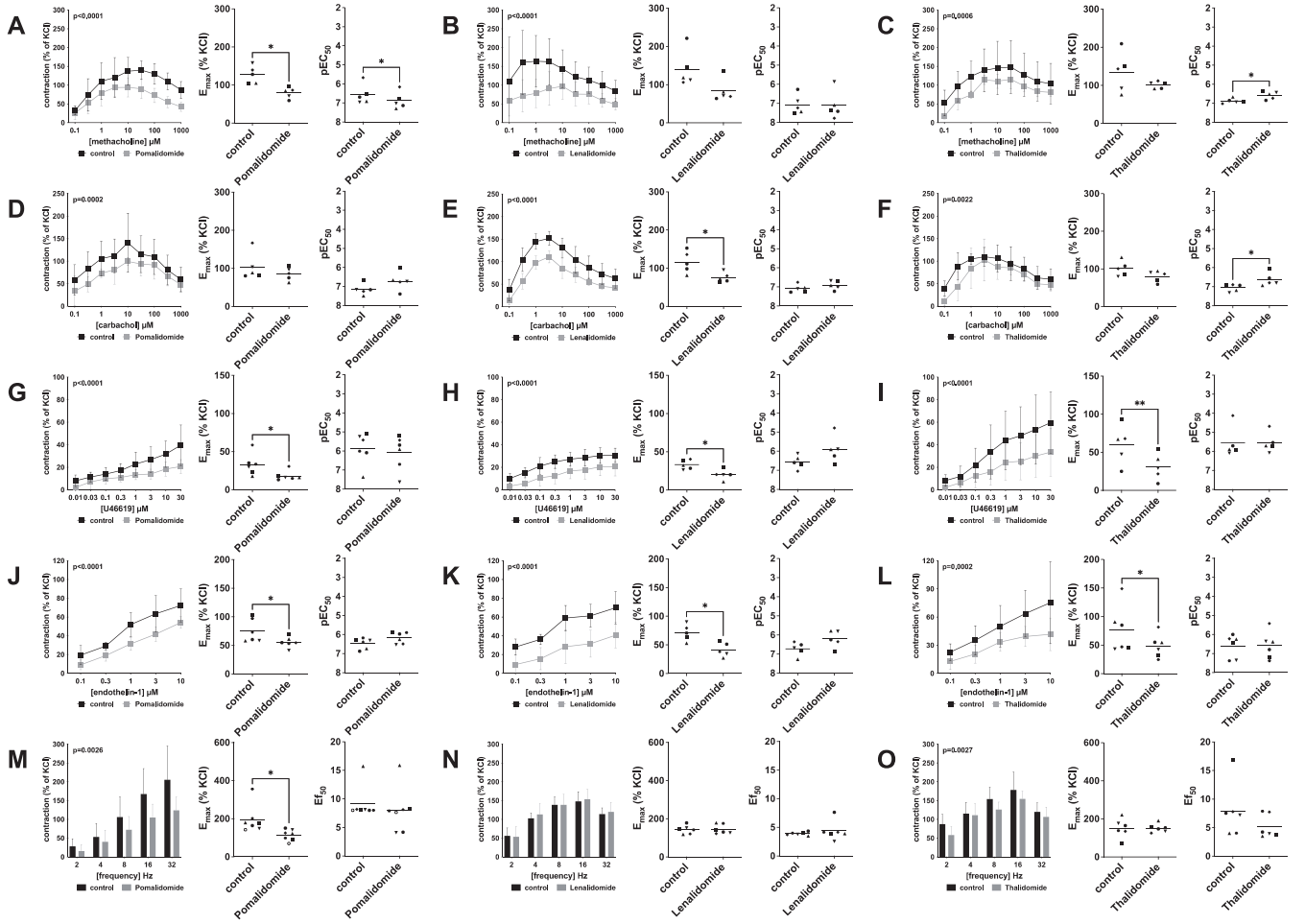

Fig. 1. Effects of IMiDs on cholinergic and non-cholinergic, and EFS-induced neurogenic contractions of human detrusor tissues.

71 [54−89] % of KCl-induced contractions in controls and to 42 [26−57] % of KCl-induced contractions after application of lenalidomide (MD 30 [6−54] %, p=0.0253; Fig. 1K), and thalidomide, amounting to 77 [34−120] % of KCl-induced contractions in controls and to 48 [27−70] % of KCl-induced contractions after application of thalidomide (MD 28 [5−52] %, p=0.0280; Fig. 1L). EC_{50} values remained unchanged for endothelin-1-induced contractions.

3.1.1.3. EFS-induced contractions. Effects of IMiDs on neurogenic contractions of human detrusor tissue were investigated using EFS. AUC in frequency response curves (2–32 Hz) for EFS-induced contractions were reduced by around one-third for pomalidomide (Fig. 1M) and by around 15 % for thalidomide (Fig. 1O), while there was no inhibitory effect using lenalidomide (Fig. 1N). While E_{max} was reduced by pomalidomide, amounting to 195 [127−264] % of KCl-induced contractions in controls and to 114 [88−141] % of KCl-induced contractions after application of pomalidomide (MD 81 [4−158] %, p=0.0425; Fig. 1M), it remained unchanged for thalidomide and lenalidomide. EC_{50} values remained unchanged for EFS-induced contractions.

Cholinergic contractions were induced by the m-cholinreceptor agonists methacholine (A-C), and carbachol (D-F), while non-cholinergic contractions were induced by thromboxane A_2 analog U46619 (G-I) and endothelin-1 (J-L), and neurogenic contraction was induced by electric field stimulation (EFS) (M-O), after addition of pomalidomide (5 µM), lenalidomide (20 µM), and thalidomide (100 µM), or DMSO for controls. To eliminate heterogeneities due to individual variations, or varying smooth muscle content, tensions have been expressed as percentages (%) of contraction by highmolar KCl, being assessed before application of inhibitors or DMSO. Each experiment used strips from different patients (n=82), and data are graphed as means ± SD from n=5 different patients for (A)-(F), n=6 different patients for (G), n=5 different patients for (H), n=5 other patients for (I), n=6 different patients for (J), n=5 different patients for (K), n=6 different patients for (L), n=7 different patients for (M), n=6 different patients for (N), and n=6 other patients for (O) per individual series. Tissue from each patient was allocated to the control and drug group examined in the same experiment, resulting in paired groups and identical group sizes in each diagram. Overall p values reflect comparison in two-way ANOVA between treatment and control groups (p values for whole groups in inserts). All single E_{max} values (left) with pEC_{50} values and Ef_{50} values (right) for agonist-induced and EFS-induced contractions, respectively, are shown in scatter plots next to their corresponding concentration-response curves (* $p<0.05$, ** $p<0.01$, calculated by two-tailed Student's t-test).

3.1.2. Concentration-dependent effects of IMiDs on methacholine- and EFS-induced contractions of human bladder detrusor tissues

.

3.1.2.1. Pomalidomide. Human detrusor smooth muscle contraction was induced by the cholinergic agonist methacholine, and neurogenic contractions were induced using EFS, following incubation with pomalidomide (at 50 µM, 500 nM, and 50 nM), lenalidomide (at 200 µM, 2 µM, and 200 nM), and thalidomide (at 1 mM, 10 µM, and 1 µM), or equal amounts of DMSO for controls.

Methacholine-induced contractions and AUC in concentration

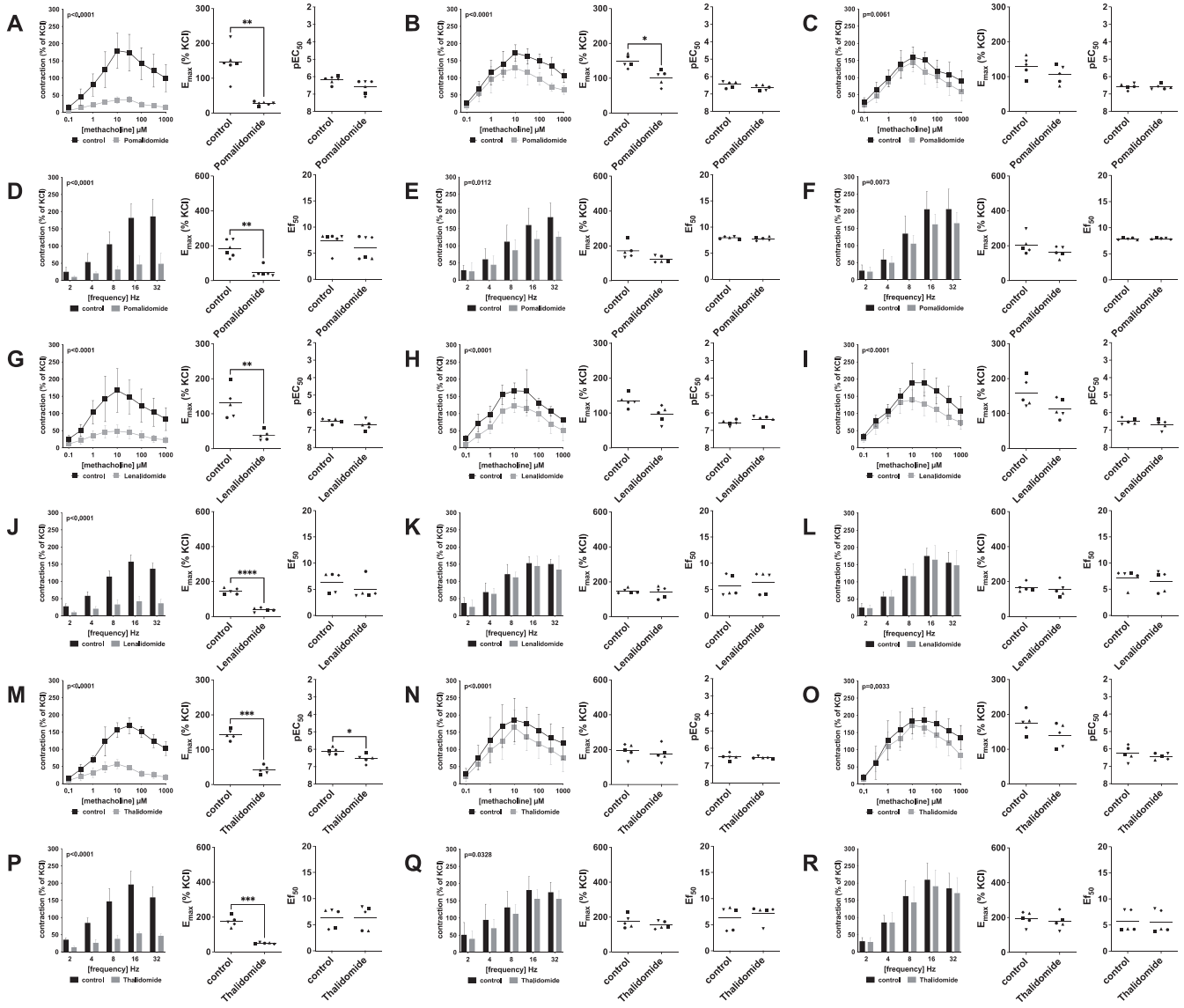

Fig. 2. Concentration-dependent effects of IMiDs on methacholine and EFS-induced contractions of human bladder detrusor tissues.

response curves (0.1–1000 µM) were reduced by around 80 %, 30 %, and 20 %, following incubation with pomalidomide at 50 µM, 500 nM, and 50 nM, respectively (Fig. 2A-C, Table 2 A). E_{max} was reduced by pomalidomide at 50 µM final concentration, amounting to 145 [98−193] % of KCl-induced contractions in controls and to 27 [22−33] % of KCl-induced contractions after application of pomalidomide (MD 118 [70−166], p=0.0014; Fig. 2A), and at 500 nM final concentration, amounting to 148 [125−170] % of KCl-induced contractions in controls and to 101 [75−128] % of KCl-induced contractions after application of pomalidomide (MD 47 [15−78], p=0.0154; Fig. 2B). EC_{50} values for methacholine remained unchanged, following incubation with pomalidomide at 50 µM, 500 nM, and 50 nM, respectively (Fig. 2A-C).

AUC in frequency response curves (2–32 Hz) for EFS-induced contractions were reduced by around 70 %, 25 %, and 20 % following incubation with pomalidomide at 50 µM, 500 nM, and 50 nM, respectively (Fig. 2D-F, Table 2 A). E_{max} was reduced by pomalidomide only at 50 µM final concentration, amounting to 182 [132−232] % of KCl-induced contractions in controls and to 47 [17−76] % of KCl-induced contractions after application of pomalidomide (MD 136 [68−204], p=0.0037; Fig. 2D). EC_{50} values for neurogenic contractions remained unchanged, following incubation with pomalidomide at 50 µM, 500 nM, and 50 nM, respectively (Fig. 2D-F).

3.1.2.2. Lenalidomide. Methacholine-induced contractions and AUC in concentration response curves (0.1–1000 µM) were reduced by around 70 %, 30 %, and 25 %, following incubation with lenalidomide at 200 µM, 2 µM, and 200 nM, respectively (Fig. 2G-I, Table 2B). E_{max} was reduced by lenalidomide only at 200 µM final concentration, amounting to 130 [75−186] % of KCl-induced contractions in controls and to 38 [21−55] % of KCl-induced contractions after application of lenalidomide (MD 92 [54−131], p=0.0026; Fig. 2G). EC_{50} values for methacholine remained unchanged, following incubation with lenalidomide at 200 µM, 2 µM, and 200 nM, respectively (Fig. 2G-I).

AUC in frequency response curves (2–32 Hz) for EFS-induced contractions were reduced by around 70 % following incubation with pomalidomide only at 200 µM (Fig. 2J, Table 2B), while there was no effect following incubation at lower concentrations i.e., 2 µM (Fig. 2K), or 200 nM (Fig. 2L). E_{max} was reduced by lenalidomide only at 200 µM final concentration, amounting to 145 [123−166] % of KCl-induced contractions in controls and to 38 [24−53] % of KCl-induced contractions after application of pomalidomide (MD 136 [68−204], p=0.0037; Fig. 2D). EC_{50} values for neurogenic contractions remained unchanged, following incubation with lenalidomide at 50 µM, 500 nM, and 50 nM, respectively (Fig. 2J-L).

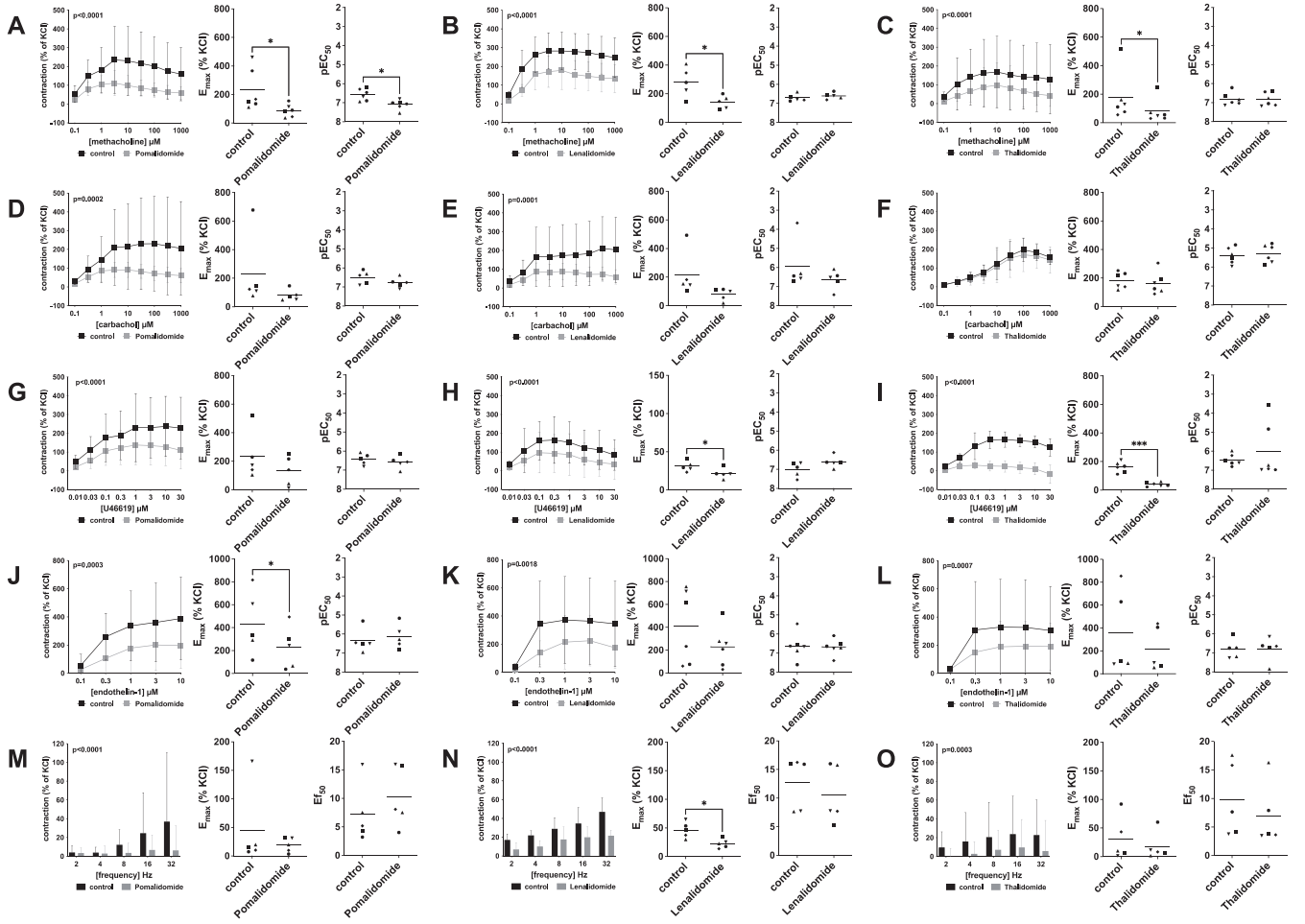

Fig. 3. Effects of IMiDs on cholinergic and non-cholinergic, and EFS-induced neurogenic contractions of porcine coronary arteries.

3.1.2.3. Thalidomide. Methacholine-induced contractions and AUC in concentration response curves (0.1–1000 μM) were reduced by around 70 %, 25 %, and 15 %, following incubation with thalidomide at 1 mM, 10 μM, and 1 μM, respectively (Fig. 2M-O, Table 2 C). E_{max} was reduced by thalidomide only at 1 mM final concentration, amounting to 143 [126−161] % of KCl-induced contractions in controls and to 42 [27−57] % of KCl-induced contractions after application of thalidomide (MD 101 [69−134], p=0.0010; Fig. 2M). EC_{50} values for methacholine remained unchanged, following incubation with thalidomide at 1 mM, 10 μM, and 1 μM, respectively (Fig. 2M-O).

AUC in frequency response curves (2–32 Hz) for EFS-induced contractions were reduced by around 70 %, and 20 % following incubation with thalidomide at 1 mM and 10 μM, respectively (Fig. 2P and Fig. 2Q, Table 2 C), while there was no effect following incubation at the lowest concentration i.e., 1 μM (Fig. 2R). E_{max} was reduced by thalidomide only at 1 mM final concentration, amounting to 174 [137−211] % of KCl-induced contractions in controls and to 50 [45−55] % of KCl-induced contractions after application of thalidomide (MD 124 [85−164], p=0.0010; Fig. 2P). EC_{50} values for neurogenic contractions remained unchanged, following incubation with thalidomide at 1 mM, 10 μM, and 1 μM, respectively (Fig. 2P-R).

Cholinergic contractions were induced by the m-cholinergic receptor agonist methacholine, and neurogenic contractions were induced using EFS, following incubation with pomalidomide at 50 μM (A and D), 500 nM (B and E), and 50 nM (C and F), lenalidomide at 200 μM (G and J), 2 μM (H and K), and 200 nM I and L), and thalidomide at 1 mM (M and P), 10 μM (N and Q), and 1 μM O and R), or equal amounts of DMSO for controls. To eliminate heterogeneities due to individual variations, or varying smooth muscle content, tensions have been expressed as percentages (%) of contraction by highmolar KCl, being assessed before application of inhibitors or DMSO. Each experiment used strips from different patients (n=92), and data are graphed as means ± SD from n=6 different patients for (A), n=5 different patients for (B), n=5 other patients for (C), n=6 different patients for (D), and n=5 different patients for (*E*)-(R) per individual series. Tissue from each patient was allocated to the control and drug group examined in the same experiment, resulting in paired groups and identical group sizes in each diagram. Overall p values reflect comparison in two-way ANOVA between treatment and control groups (p values for whole groups in inserts). All single E_{max} values (left) with pEC_{50} values and Ef_{50} values (right) for agonist-induced and EFS-induced contractions, respectively, are shown in scatter plots next to their corresponding concentration-response curves (* p<0.05, ** p<0.01, *** p<0.001, **** p<0.0001, calculated by two-tailed Student's t-test).

3.1.3. *Effects of IMiDs on contractions of porcine coronary arteries*

3.1.3.1. Cholinergic contractions. Porcine coronary artery vasoconstriction was induced by the cholinergic agonists carbachol and methacholine following incubation with pomalidomide (5 μM), lenalidomide (20 μM), and thalidomide (100 μM), or equal amounts of DMSO for controls. AUC for methacholine-induced contractions were reduced by around 50 % for all three IMiDs (Fig. 3A-C). E_{max} was reduced by pomalidomide, lenalidomide, and thalidomide, amounting to 231 [79−384] % of KCl-induced contractions in controls and to 87 [41−134] % of KCl-induced contractions after application of pomalidomide (MD

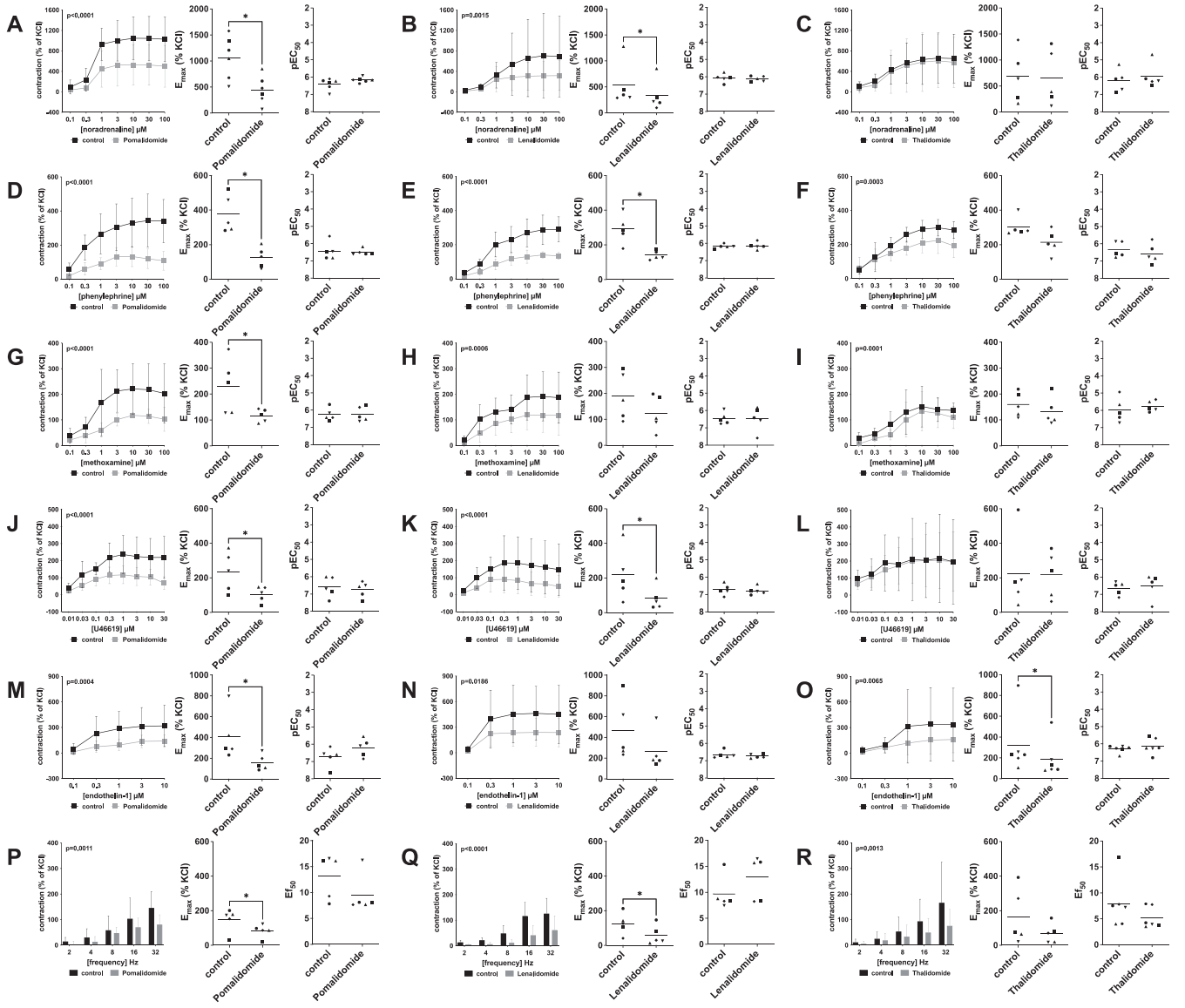

Fig. 4. Effects of IMiDs on adrenergic and non-adrenergic, and EFS-induced neurogenic contractions of porcine renal interlobar arteries.

144 [22–265] %, p=0.0287; Fig. 3A), to 279 [150–408] % of KCl-induced contractions in controls and to 140 [82–198] % of KCl-induced contractions after application of lenalidomide (MD 139 [41–238] %, p=0.0171; Fig. 3B), and to 175 [-4–353] % of KCl-induced contractions in controls and to 82 [-7–170] % of KCl-induced contractions after application of thalidomide (MD 93 [2–184] %, p=0.0465; Fig. 3C), respectively. EC_{50} values for methacholine were decreased by pomalidomide, reflected by increases of pEC_{50} values from 6.6 [6.2–6.9] in controls to 7.1 [6.8–7.4] after application of pomalidomide (MD 0.5 [0.2–0.9]; p=0.0129; Fig. 3A), while EC_{50} values remained unchanged following incubation with thalidomide, or lenalidomide, respectively.

AUC in concentration response curves (0.1–1000 µM) for carbachol-induced contractions were reduced by around 50 % for pomalidomide (Fig. 3D) and lenalidomide (Fig. 3E), while there was no significant inhibition following incubation with thalidomide. E_{max} and pEC_{50} remained unchanged following incubation with either IMiD.

3.1.3.2. Non-cholinergic contractions. All three IMiDs inhibited non-cholinergic contractions induced by U46619 and reduced AUC in concentration response curves (0.01–30 µM) by half for pomalidomide (Fig. 3G) and lenalidomide (Fig. 3H), and around 80 % for thalidomide (Fig. 3I). E_{max} was reduced by lenalidomide, amounting to 140 [13–267] % of KCl-induced contractions in controls and to 89 [-14–191] % of KCl-induced contractions after application of lenalidomide (MD 52 [13–90] %, p=0.0206; Fig. 3H), and thalidomide, amounting to 161 [122–200] % of KCl-induced contractions in controls and to 40 [25–56] % of KCl-induced contractions after application of thalidomide (MD 121 [81–160] %, p=0.0005; Fig. 3I), respectively, while remaining unchanged following incubation with pomalidomide. EC_{50} values remained unchanged for U46619-induced contractions.

Endothelin-1-induced contractions were inhibited and AUC in concentration response curves (0.1–10 µM) were reduced by around 50 % for all three IMiDs (Fig. 3J-L). E_{max} was reduced by pomalidomide, amounting to 434 [90–778] % of KCl-induced contractions in controls and to 228 [-3–458] % of KCl-induced contractions after application of pomalidomide (MD 206 [28–385] %, p=0.0325; Fig. 3L), while remaining unchanged for thalidomide, and lenalidomide, respectively. EC_{50} values remained unchanged for endothelin-1-induced contractions.

3.1.3.3. EFS-induced contractions. Effects of IMiDs on neurogenic contractions of porcine coronary arteries were examined using EFS. EFS-induced contractions were inhibited and AUC in frequency response

curves (2–32 Hz) were reduced by half for pomalidomide (Fig. 3M) and lenalidomide (Fig. 3N), and by around 75 % for thalidomide (Fig. 3O). While E_{max} was reduced by lenalidomide, amounting to 46 [29−63] % of KCl-induced contractions in controls and to 23 [13−32] % of KCl-induced contractions after application of lenalidomide (MD 24 [6−41] %, p=0.0208; Fig. 3N), it remained unchanged for thalidomide and pomalidomide. EC_{50} values remained unchanged for EFS-induced contractions.

Cholinergic contractions were induced by the m-cholinreceptor agonists methacholine (A-C), and carbachol (D-F), while non-cholinergic contractions were induced by thromboxane A_2 analog U46619 (G-I) and endothelin-1 (J-L), and neurogenic contraction was induced by electric field stimulation (EFS) (M-O), after addition of pomalidomide (5 μM), lenalidomide (20 μM), and thalidomide (100 μM), or DMSO for controls. To eliminate heterogeneities due to individual variations, or varying smooth muscle content, tensions have been expressed as percentages (%) of contraction by highmolar KCl, being assessed before application of inhibitors or DMSO. Each experiment used strips from different patients (n=80), and data are graphed as means ± SD SD from n=6 different animals for (A), n=5 different animals for (B), n=6 different animals for (C), n=5 different animals for (D), n=5 other animals for (E), n=6 different animals for (F), n=5 different animals for (G), n=5 other animals for (H), n=6 different animals for (I), n=5 different animals for (J), n=6 different animals for (K), and n=5 different animals for (L)-(O) per individual series. Tissue from each animal was allocated to the control and drug group examined in the same experiment, resulting in paired groups and identical group sizes in each diagram. Overall p values reflect comparison in two-way ANOVA between treatment and control groups (p values for whole groups in inserts). All single E_{max} values (left) with pEC_{50} values and Ef_{50} values (right) for agonist-induced and EFS-induced contractions, respectively, are shown in scatter plots next to their corresponding concentration-response curves (* $p<0.05$, *** $p<0.001$, calculated by two-tailed Student's t-test).

3.1.4. Effects of IMiDs on contractions of porcine renal interlobar arteries

3.1.4.1. Adrenergic contractions. Porcine coronary artery vasoconstriction was induced by the adrenergic agonists noradrenaline, phenylephrine, and methoxamine following incubation with pomalidomide (5 μM), lenalidomide (20 μM), and thalidomide (100 μM), or equal amounts of DMSO for controls. Noradrenaline-induced contractions were inhibited, and AUC reduced in concentration response curves (0.1–100 μM) by around half for pomalidomide (Fig. 4A) and lenalidomide (Fig. 4B), while there was no significant inhibition following incubation with thalidomide. E_{max} was reduced by pomalidomide, and lenalidomide, amounting to 1066 [636–1497] % of KCl-induced contractions in controls and to 442 [159−726] % of KCl-induced contractions after application of pomalidomide (MD 624 [154–1094] %, p=0.0190; Fig. 4A), and to 532 [6–1058] % of KCl-induced contractions in controls and to 331 [-42−705] % of KCl-induced contractions after application of lenalidomide (MD 201 [36−366] %, p=0.0267; Fig. 4B), respectively, while E_{max} remained unchanged following incubation with thalidomide. EC_{50} values remained unchanged for noradrenaline-induced contractions.

Phenylephrine-induced contractions were inhibited and AUC in concentration response curves (0.1–100 μM) were reduced by around 50 % for pomalidomide (Fig. 4D) and lenalidomide (Fig. 4E), and around one-fourth for thalidomide (Fig. 4F). E_{max} was reduced by pomalidomide, and lenalidomide, amounting to 376 [242−509] % of KCl-induced contractions in controls and to 127 [54−201] % of KCl-induced contractions after application of pomalidomide (MD 248 [48−449] %, p=0.0264; Fig. 4D), and to 292 [190−393] % of KCl-induced contractions in controls and to 141 [108−174] % of KCl-induced contractions after application of lenalidomide (MD 151 [46−255] %, p=0.0163; Fig. 4E), respectively, while E_{max} remained unchanged following incubation with thalidomide. EC_{50} values remained unchanged for phenylephrine-induced contractions.

Methoxamine-induced contractions were inhibited and AUC in concentration response curves (0.1–100 μM) were reduced by around half for pomalidomide (Fig. 4G) and lenalidomide (Fig. 4H), and around one-third for thalidomide (Fig. 4F). E_{max} was reduced only by pomalidomide, amounting to 231 [101−361] % of KCl-induced contractions in controls and to 117 [86−148] % of KCl-induced contractions after application of pomalidomide (MD 114 [13−215] %, p=0.0349; Fig. 4G), while E_{max} remained unchanged following incubation with thalidomide, or lenalidomide. EC_{50} values remained unchanged for methoxamine-induced contractions.

3.1.4.2. Non-adrenergic contractions. Contractions induced by U46619 were inhibited and AUC in concentration response curves (0.01–30 μM) were reduced by around 50 % for pomalidomide (Fig. 4J) and lenalidomide (Fig. 4K), while there was no significant inhibition following incubation with thalidomide (Fig. 4L). E_{max} was reduced by pomalidomide, amounting to 235 [92−377] % of KCl-induced contractions in controls and to 105 [50−160] % of KCl-induced contractions after application of pomalidomide (MD 130 [39−220] %, p=0.0165; Fig. 4J), and by lenalidomide, amounting to 218 [34−401] % of KCl-induced contractions in controls and to 83 [-2−167] % of KCl-induced contractions after application of lenalidomide (MD 134 [27−242] %, p=0.0256; Fig. 4K), respectively, while remaining unchanged following incubation with thalidomide. EC_{50} values remained unchanged for U46619-induced contractions. Endothelin-1-induced contractions were inhibited and AUC in concentration response curves (0.1–10 μM) were reduced around half for all three IMiDs (Fig. 4M-O). E_{max} was reduced by pomalidomide, amounting to 406 [122−690] % of KCl-induced contractions in controls and to 159 [64−253] % of KCl-induced contractions after application of pomalidomide (MD 247 [31−464] %, p=0.0339; Fig. 4M), and thalidomide, amounting to 320 [19−621] % of KCl-induced contractions in controls and to 187 [1−373] % of KCl-induced contractions after application of thalidomide (MD 133 [12−255] %, p=0.0370; Fig. 4O), while remaining unchanged for lenalidomide. EC_{50} values remained unchanged for endothelin-1-induced contractions.

3.1.4.3. EFS-induced contractions. Effects of IMiDs on neurogenic contractions of porcine renal interlobar arteries were investigated using EFS. EFS-induced contractions were inhibited, and AUC in frequency response curves (2–32 Hz) were reduced by around half for pomalidomide (Fig. 4P) and thalidomide (Fig. 4R), and by two-thirds for lenalidomide (Fig. 4Q). While E_{max} was reduced by pomalidomide, amounting to 148 [65−231] % of KCl-induced contractions in controls and to 83 [35−131] % of KCl-induced contractions after application of pomalidomide (MD 65 [21−110] %, p=0.0152; Fig. 4P), and by lenalidomide, amounting to 125 [48−202] % of KCl-induced contractions in controls and to 59 [-9−128] % of KCl-induced contractions after application of lenalidomide (MD 66 [4−127] %, p=0.0409; Fig. 4Q), it remained unchanged for thalidomide. EC_{50} values remained unchanged for EFS-induced contractions.

Adrenergic contractions were induced by α_1-unselective agonist noradrenaline (A-C), α_{1A}- and α_{1B}-selective agonist phenylephrine (D-F), and α_{1A}-selective agonist methoxamine (G-I), while non-adrenergic contractions were induced by thromboxane A_2 analog U46619 (J-L) and endothelin-1 (M-O), and neurogenic contraction was induced by electric field stimulation (EFS) (P-R), after addition of pomalidomide (5 μM), lenalidomide (20 μM), and thalidomide (100 μM), or DMSO for controls. To eliminate heterogeneities due to individual variations, or varying smooth muscle content, tensions have been expressed as percentages (%) of contraction by highmolar KCl, being assessed before application of inhibitors or DMSO. Each experiment used strips from

different animals (n=92), and data are graphed as means ± SD from n=6 different animals for (A), n=5 different animals for (B)-(N), n=6 different animals for (O), and n=5 different animals for (P)-(R) per individual series. Tissue from each animal was allocated to the control and drug group examined in the same experiment, resulting in paired groups and identical group sizes in each diagram. Overall p values reflect comparison in two-way ANOVA between treatment and control groups (p values for whole groups in inserts). All single E_{max} values (left) with pEC_{50} values and Ef_{50} values (right) for agonist-induced and EFS-induced contractions, respectively, are shown in scatter plots next to their corresponding concentration-response curves (* $p<0.05$, calculated by two-tailed Student's t-test).

3.2. Cell culture studies

3.2.1. Effects of IMiDs on proliferation of HBdSM cells

IMiDs reduced the proliferation rate in HBdSM cells (Fig. 5). After exposure to pomalidomide for 24 hours, the proliferation rate was reduced to 9.4 [7.8–11.1] %, 6.7 [5.8–8.0] %, and 5.4 [4.9–5.8] % by 2.5 μM, 5 μM, and 10 μM pomalidomide, respectively, while 21 [15.5–25.5] % of solvent-treated cells (DMSO) showed proliferation (p=0.0101, p=0.0032, and p=0.0031 for 2.5 μM, 5 μM, and 10 μM pomalidomide vs. control, respectively; Fig. 5A). After exposure to lenalidomide for 24 hours, the proliferation rate was reduced to 8.5 [6.6–10.3] %, 5.7 [4.7–6.8] %, and 4.5 [2.5–6.4] % by 5 μM, 10 μM, and 30 μM lenalidomide, respectively, while 20 [18.0–22.8] % of solvent-treated cells (DMSO) showed proliferation (p=0.0001, p=0.0002, and p=0.0011 for 5 μM, 10 μM, and 30 μM lenalidomide vs. control, respectively; Fig. 5B). After exposure to thalidomide for 24 hours, the proliferation rate was reduced to 8.7 [6.7–10.7] %, 5.7 [4.4–7.0] %, and 3.9 [3.7–4.1] % by 10 μM, 30 μM, and 100 μM thalidomide, respectively, while 23 [19.7–27.1] % of solvent-treated cells (DMSO) showed proliferation (p=0.0021, p=0.0015, and p=0.0004 for 10 μM, 30 μM, and 100 μM thalidomide vs. control, respectively; Fig. 5C).

Shown are the percentages of proliferation (means ± SD) for each concentration and inhibitor i.e., pomalidomide at 2.5, 5, and 10 μM (A), lenalidomide at 5, 10, and 30 μM (B), and thalidomide at 10, 30, and 100 μM (C) after 24 hours, using cell cultures from n=5 independent experiments for each concentration. The cells were either allocated to a control (DMSO) or inhibitor group (* $p<0.05$, ** $p<0.01$, *** $p<0.001$), and incubated for 24 hours. Proliferating cells were detected by EdU staining and counterstaining of all nuclei with DAPI, followed by fluorescence microscopy, resulting in blue-colored nuclei for non-proliferating cells and red nuclei for proliferating cells. Shown are exemplary images of cell proliferation after 24 hours (left), quantification of all experiments (right) from all five experiments.

3.2.2. Effects of IMiDs on colony formation of HBdSM cells

IMiDs reduced colony formation in HBdSM cells in a concentration-dependent manner (Fig. 6). The number of colonies per well amounted to 30 [25−34] colonies, 25 [20−30] colonies and 22 [19−24] colonies with 2.5 μM, 5 μM, and 10 μM pomalidomide, respectively, compared to 46 [40−53] colonies for solvent-treated controls ($p<0.0001$ for 2.5 μM, 5 μM, and 10 μM pomalidomide vs. control after 168 hours, respectively; Fig. 6 A). The number of colonies per well amounted to 32 [23−42] colonies, 29 [19−38] colonies and 23 [14−32] colonies with 5 μM, 10 μM, and 30 μM lenalidomide, respectively, compared to 51 [41−61] colonies for solvent-treated controls (p=0.0035, p=0.0008, and $p<0.0001$ for 5 μM, 10 μM, and 30 μM lenalidomide vs. control after 168 hours, respectively; Fig. 6B). The number of colonies per well amounted to 33 [30−38] colonies, 28 [26−30] colonies and 26 [24−29] colonies with 10 μM, 30 μM, and 100 μM thalidomide, respectively, compared to 50 [43−57] colonies for solvent-treated controls ($p<0.0001$ for 10 μM, 30 μM, and 100 μM thalidomide vs. control after 168 hours, respectively; Fig. 6 C).

Shown are the absolute numbers of colonies (n) after 168 h (single values with means) from series using cell cultures from n=5 independent experiments for each concentration and inhibitor i.e., pomalidomide at 2.5, 5, and 10 μM (A), lenalidomide at 5, 10, and 30 μM (B), and thalidomide at 10, 30, and 100 μM (C). The cells were either allocated to a control (DMSO) or inhibitor group (** $p<0.01$, *** $p<0.001$, **** $p<0.0001$), and incubated for 168 hours. Shown are exemplary images of colony formation after 168 hours (left), and quantification of all experiments (right).

3.2.3. Effects of IMiDs on viability of HBdSM cells

Viability of HBdSM cells was reduced following exposure to IMiDs, which is depicted in Fig. 7 as optical density (OD), with respective p-values given in the scatterplots. If referred to corresponding controls, we observed a statistically significant decrease in viability following exposure to pomalidomide only at the higher concentrations, and following longer incubation periods than compared to thalidomide or lenalidomide, with 19 [15−22] % for 10 μM after 24 hours, 16 [6−26] %, and 48 [44−52] %, for 5 μM and 10 μM after 48 hours, respectively, and 8 [6−11] %, and 54 [50−59] %, for 5 μM and 10 μM after 72 hours, respectively (Fig. 7A). Following exposure to lenalidomide we observed a statistically significant and stronger decrease in viability than compared to thalidomide with 55 [52−58] %, 64 [60−67] %, and 78 [76−81] % after 24 hours, 25 [21−30] %, 28 [22−34] %, and 75 [73−77] % after 48 hours, and 13 [9−18] %, 20 [16−24] %, and 61 [55−67] % after 72 hours, for 5 μM, 10 μM, and 30 μM, respectively (Fig. 7B). Following exposure to thalidomide we observed statistically significant decreases in viability following exposure to thalidomide after 24 hours of 19 [14−24] %, 42 [37−46] %, and 50 [42−58] %, after 48 hours of 16 [8−23] %, 28 [21−35] %, and 51 [44−58] %, and after 72 hours of 7 [3−11] %, 12 [8−16] %, and 37 [33−40] %, for 10 μM, 30 μM, and 100 μM, respectively (Fig. 7C). Together, the decline in viability was concentration-dependent, but not progressive and remained incomplete even at the highest concentration.

To assess viability, a CCK-8 assay was performed, and values are graphed as optical density (OD) from series using cell cultures from n=5 independent experiments for each concentration, inhibitor, i.e., pomalidomide at 2.5, 5, and 10 μM (A), lenalidomide at 5, 10, and 30 μM (B), and thalidomide at 10, 30, and 100 μM (C), and time. The cells were either allocated to a control (DMSO) or inhibitor group (** $p<0.01$, *** $p<0.001$, **** $p<0.0001$), and incubated for 24, 48, and 72 hours. Shown are the quantifications of all experiments as optical density (OD; single values with means).

3.2.4. Effects of IMiDs on apoptosis and cell death of HBdSM cells

IMiDs increased the relative number of dead cells. For pomalidomide this increase was concentration-dependent at 10.1 [9.1–11.1] %, 11.8 [10.4–13.3] %, and 16.2 [15.0–17.3] % after incubation with 2.5 μM, 5 μM, and 10 μM of pomalidomide for 72 hours, compared to 3.0 [2.7–3.4] % for solvent-treated controls ($p<0.0001$ for 2.5 μM, 5 μM, and 10 μM pomalidomide vs. control, respectively; Fig. 8A). For lenalidomide this increase was also concentration-dependent at 5.9 [5.5–6.3] %, 8.3 [7.9–8.7] %, and 10.3 [9.8–10.8] % after incubation with 5 μM, 10 μM, and 30 μM of lenalidomide for 72 hours, compared to 3.0 [2.6–3.4] % for solvent-treated controls ($p<0.0001$ for 5 μM, 10 μM, and 30 μM lenalidomide vs. control, respectively; Fig. 8B). For thalidomide this increase was not concentration-dependent, but reached a stable plateau at 11.5 [11.0–12.0] %, 11.1 [9.6–12.7] %, and 11.1 [10.0–12.2] % after incubation with 10 μM, 30 μM, and 100 μM of thalidomide for 72 hours, compared to 3.2 [2.4–4.1] % for solvent-treated controls ($p<0.0001$ for 10 μM, 30 μM, and 100 μM thalidomide vs. control, respectively; Fig. 8C). Taken together, there was no significant increase in the relative number of cells in apoptosis for either IMiD (Fig. 8A, B, and C).

Flow cytometry was performed, after cells were allocated to a control (DMSO) or inhibitor group i.e., pomalidomide at 2.5, 5, and 10 μM (A), lenalidomide at 5, 10, and 30 μM (B), and thalidomide at 10, 30, and

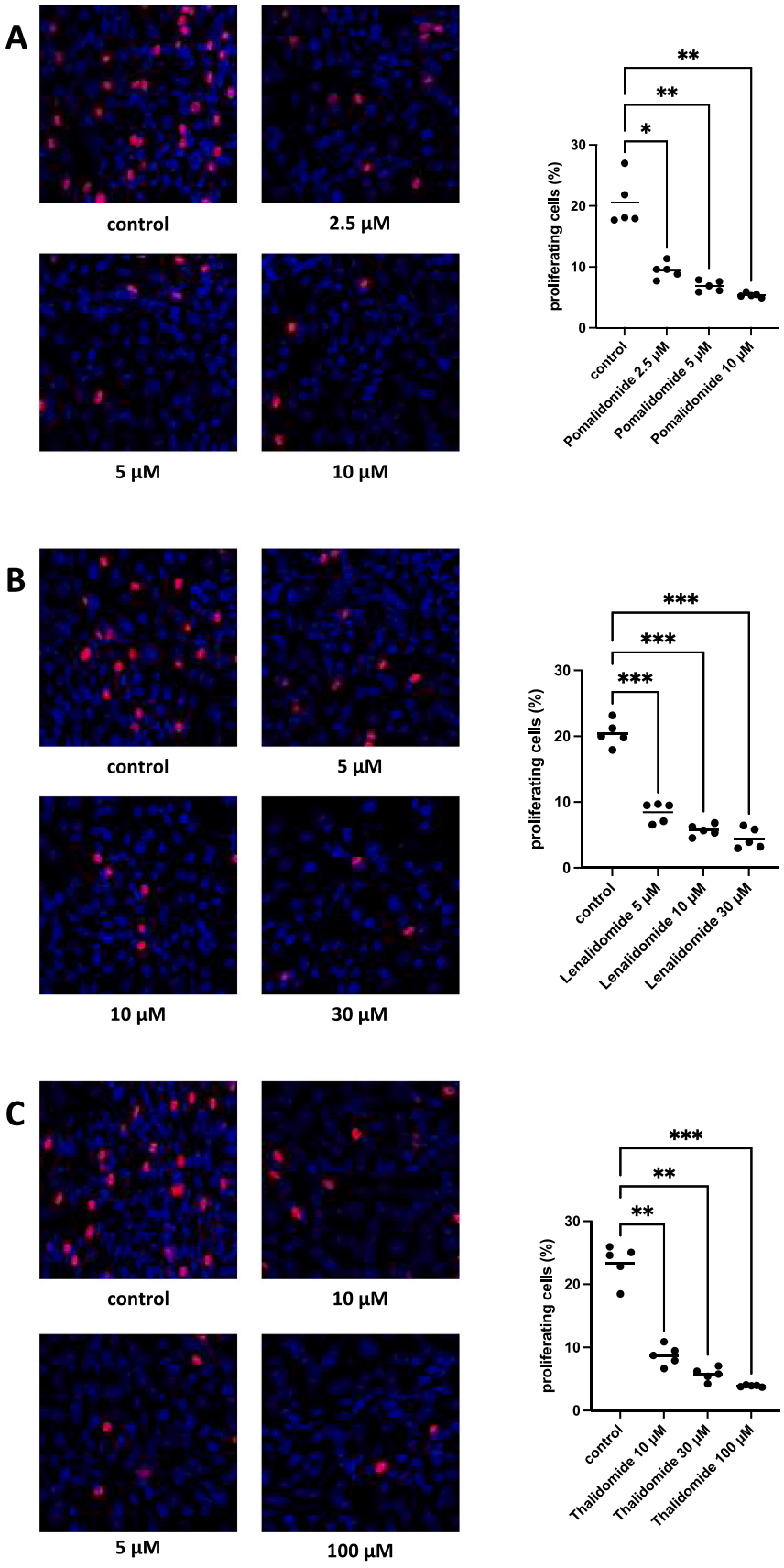

Fig. 5. Inhibition of human detrusor smooth muscle cell proliferation by IMiDs.

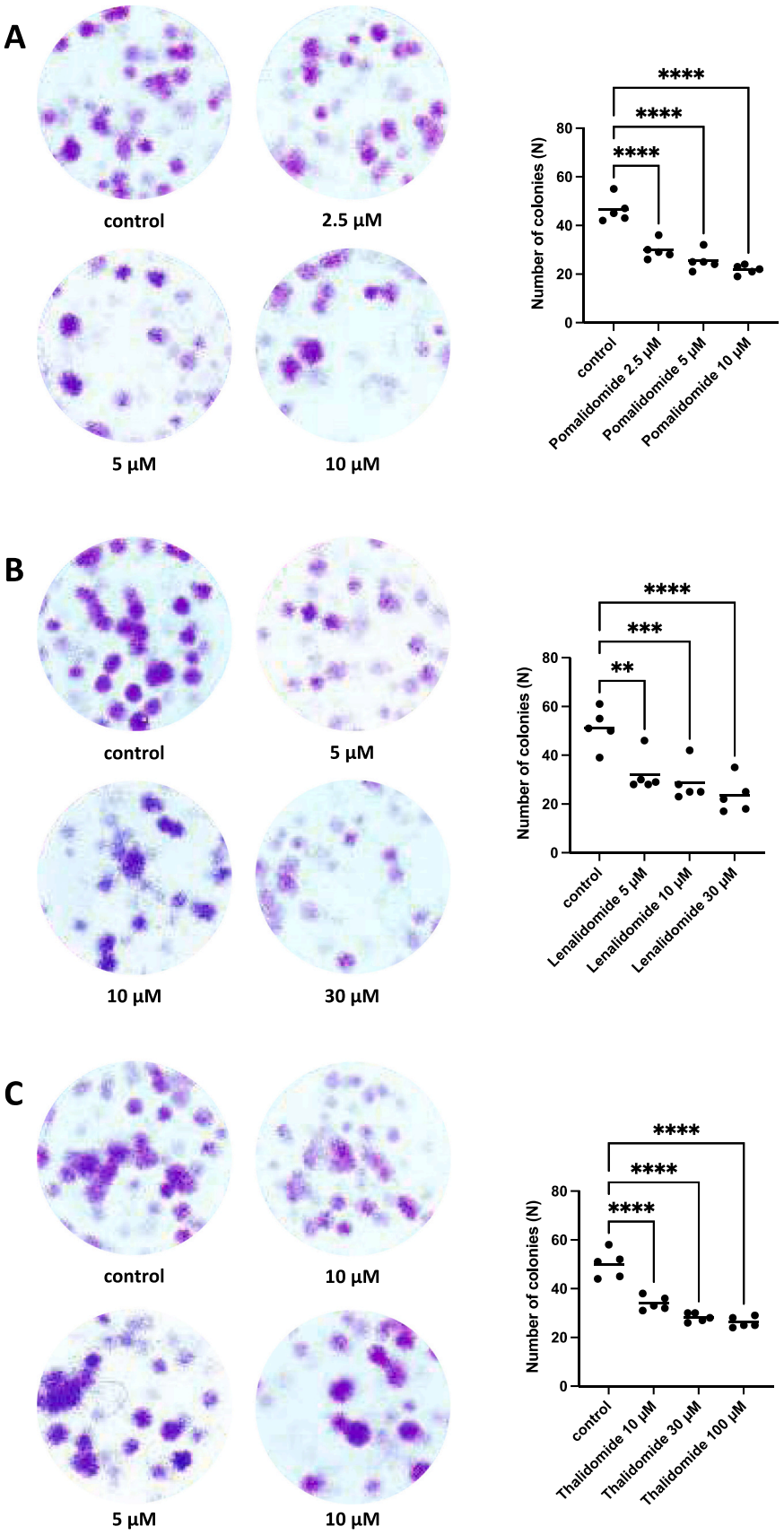

Fig. 6. Inhibition of human detrusor smooth muscle cell colony formation by IMiDs.

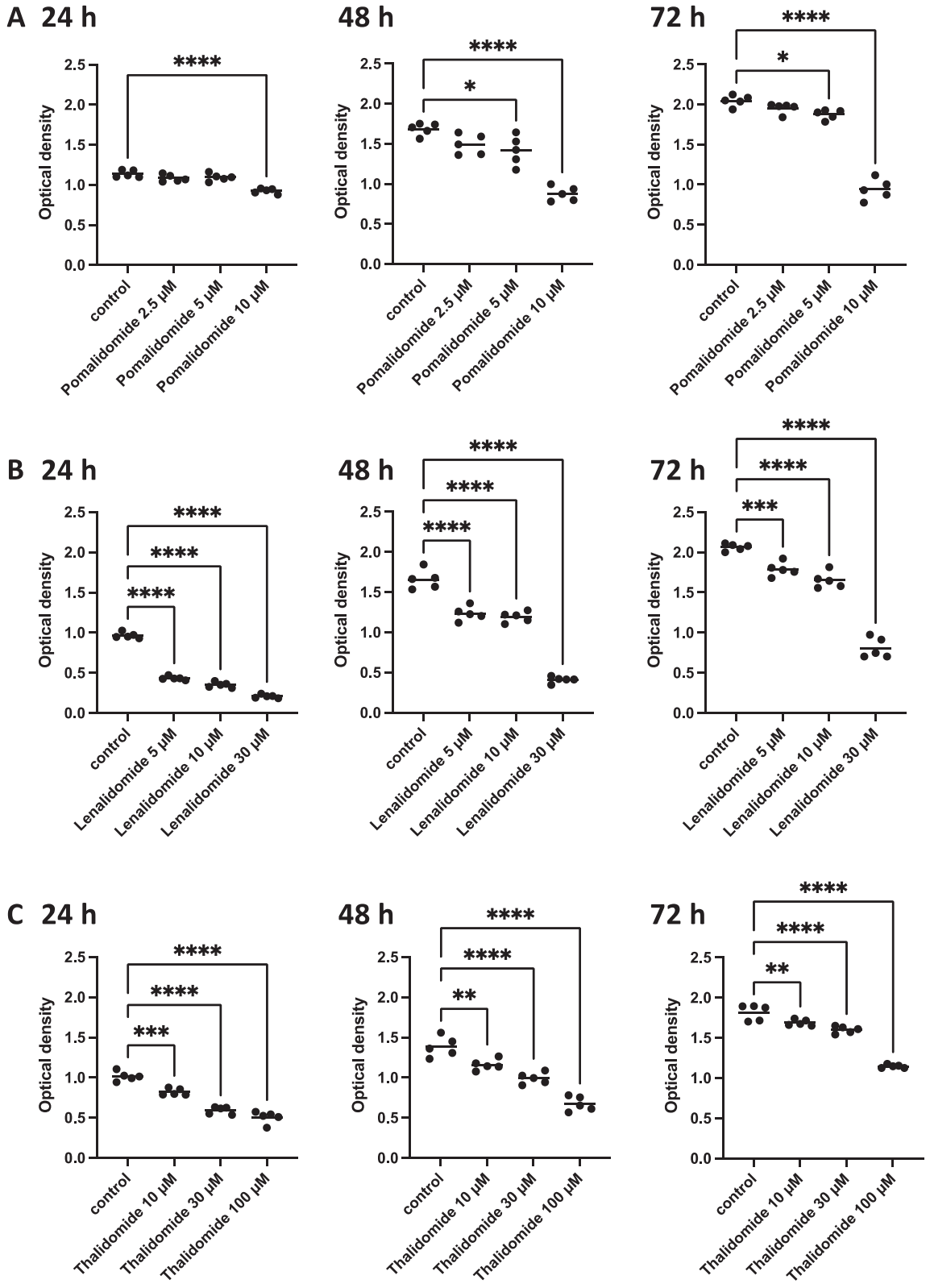

Fig. 7. Reduction of human detrusor smooth muscle cell viability by IMiDs.

100 µM (C), and treated for 72 hours (**** $p<0.0001$). Subsequently, the numbers of cells in apoptosis (annexin V-positive, 7-AAD-negative), and of dead cells (resulting from apoptosis and/or necrosis; annexin V-positive, 7-AAD-positive) were assessed by flow cytometry. Shown are representative single experiments and values are graphed as single values with means from series using cell cultures from n=5 independent experiments for each concentration and inhibitor.

3.2.5. *Effects of IMiDs on actin organization of HBdSM cells*

Actin filaments in solvent-treated control HBdSM cells showed

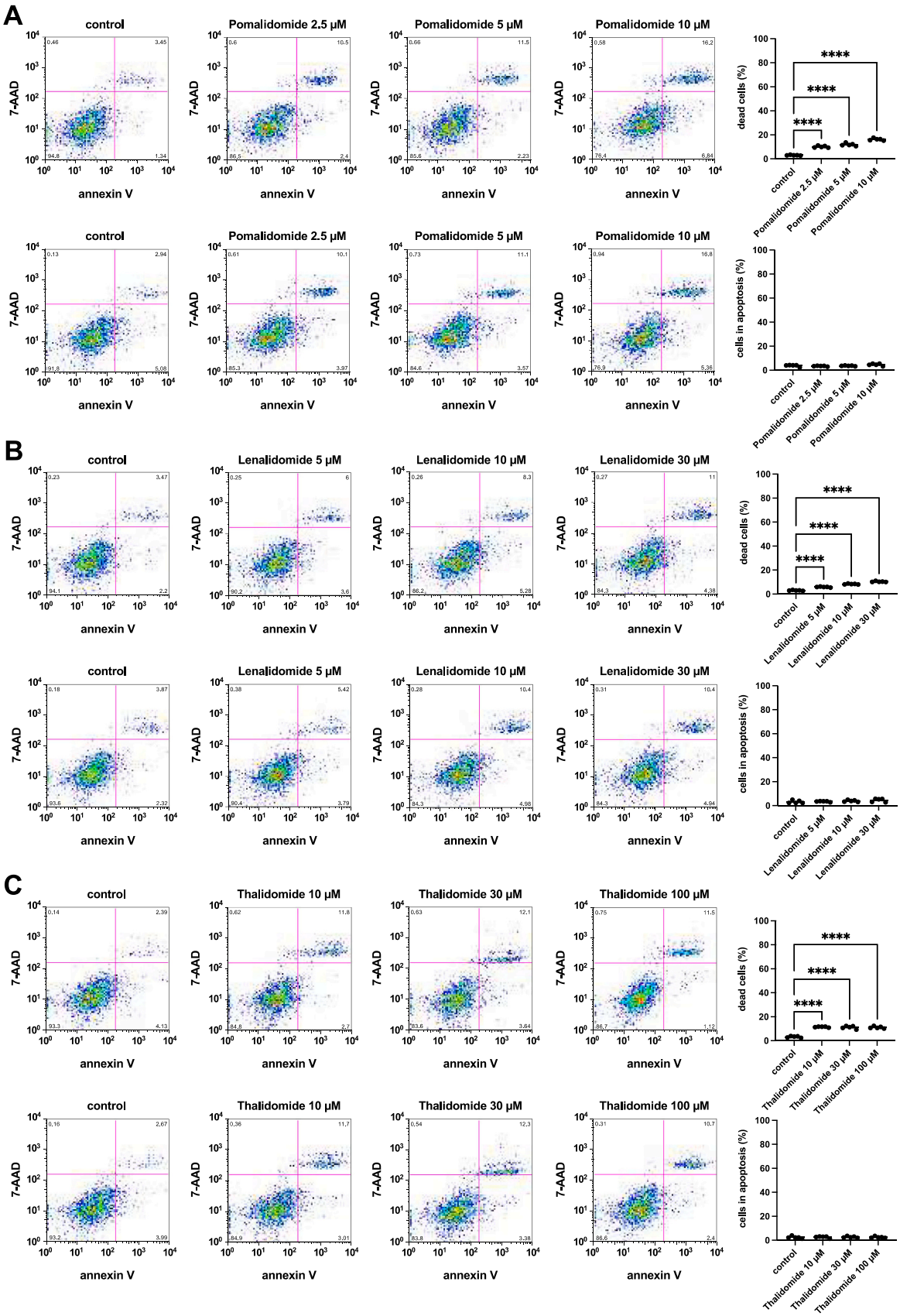

Fig. 8. Apoptosis and cell death in human detrusor smooth muscle cells after stimulation with IMiDs.

bundles of long and thin protrusions, and elongations from adjacent cells were overlapping each other (Fig. 9). IMiDs reduced the amount of polymerized actin, with consequent breakdown of actin filaments in a concentration-dependent manner after incubation for 24 hours, resulting in a loss of actin filaments. Pomalidomide caused regression of phalloidin-stained areas from 68 [65−70] % in solvent-treated control cells to 44 [38−49] %, 36 [31−40] %, and 27 [22−31] % for incubation with 2.5 μM, 5 μM, and 10 μM of pomalidomide ($p<0.0001$ for 2.5 μM, 5 μM, and 10 μM of pomalidomide vs. control, respectively; Fig. 9A). Lenalidomide caused regression of phalloidin-stained areas from 67 [61−74] % in solvent-treated control cells to 49 [39−60] %, 38 [33−43] %, and 13 [1−24] % for incubation with 5 μM, 10 μM, and 30 μM of lenalidomide ($p=0.0025$, and $p<0.0001$ for 5 μM, 10 μM, and 30 μM of lenalidomide vs. control, respectively; Fig. 9B). Thalidomide caused regression of phalloidin-stained areas from 68 [62−74] % in solvent-treated control cells to 51 [37−65] %, 20 [7−34] %, and 8 [2−14] % for incubation with 10 μM, 30 μM, and 100 μM of thalidomide ($p=0.0179$, and $p<0.0001$ for 10 μM, 30 μM, and 100 μM of thalidomide vs. control, respectively; Fig. 9C). The decline in actin-stained area was concentration-dependent for each IMiD, and obviously reached a maximum at the highest applied concentration.

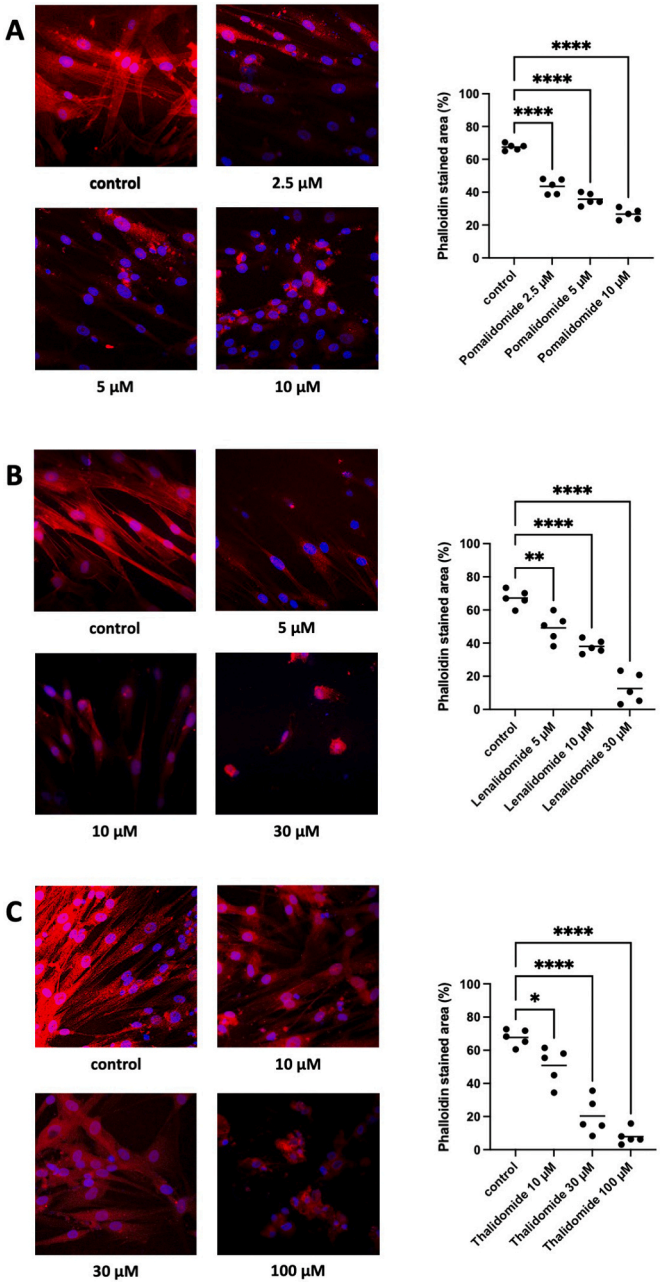

Fig. 9. Inhibition of human detrusor smooth muscle cell actin organization by IMiDs.

Shown are actin filaments, visualized by phalloidin staining, after 24 hours of exposure from series using cell cultures from n=5 independent experiments for each panel. The cells were either allocated to a control (DMSO) or inhibitor group i.e., pomalidomide at 2.5, 5, and 10 μM (A), lenalidomide at 5, 10, and 30 μM (B), and thalidomide at 10, 30, and 100 μM (C), and incubated for 24 hours. Actin filaments were visualized by phalloidin staining and fluorescence microscopy, while the nuclei were visualized using DAPI staining. Shown are individual values with means quantified as percentage (%) of phalloidin-stained area (* $p<0.05$, ** $p<0.01$, *** $p<0.001$, **** $p<0.0001$), representative single experiments from series of n=5 independent experiments for each panel (left) and the corresponding single values from all five experiments (right) for each series.

4. Discussion

Drugs prescribed for the treatment of LUTS rank among the most prescribed medications. Substance classes include antimuscarinics for storage symptoms in LUTS/OAB and β_3-adrenoceptor agonists [1,9], while 5-ARI are used for slowing down prostate growth and disease progression and α_1-blockers have recently been complemented by phosphodiesterase-5 (PDE-5) inhibitors for rapid relieve of voiding symptoms in LUTS/BPH, [3,34], reflecting the dire need for new substance classes for LUTS pharmacotherapy. European and U.S. guidelines have recently included “mixed LUTS” and, thus, have acknowledged the multifactorial and complex pathophysiology of non-neurogenic male LUTS, while offering nothing more than combinations of current monotherapies [1,35]. Acknowledging that OAB and BOO may originate as separate processes, brings with it the necessity to target a much more difficult symptom complex of LUTS in men [36]. While both symptom complexes have in common that smooth muscle contraction is a central factor in their etiology and medical treatment, both are mediated by different receptors and are characterized by differences in intracellular pathways mediating the receptor-induced contractions, together adding to the complexity of LUTS [22].

Lenalidomide and pomalidomide are both structurally similar derivatives of thalidomide, known for causing birth defects following its use as an anti-emetic in pregnant women in the 1960s [14]. However, thalidomide was re-introduced for treating ENL in 1998 by the food and drug administration (FDA), as it was noted to have anti-inflammatory and immunomodulatory effects [16–18,37,38]. With the System for Thalidomide Education and Prescribing Safety (STEPS), the manufacturing company set up a safety program [39]. IMiDs are now widely used in several diseases, including Behçet’s, Crohn’s, discoid lupus, complex pain syndrome, and rheumatoid arthritis, and continue to expand their therapeutic value [16–18,37,38]. IMiDs are an orally available and highly established and effective treatment option in multiple myeloma [15]. Thus, the translational value of thalidomide and its analogues is high – in particular, in elderly male patients, where the risk of teratogenicity does not apply.

Recent investigations showed that thalidomide, lenalidomide, and pomalidomide inhibited prostate smooth muscle contraction, and may exert regulative actions on prostatic hyperplastic growth [12,13]. Highest translational potential for new LUTS medication lies in drugs simultaneously inhibiting prostate and bladder smooth muscle contraction, and cell proliferation by using a single compound. However, data was previously limited to human prostate tissues and a line of immortalized prostate stromal cells, while data on human bladder detrusor tissues and HBdSM cells, and peripheral vasoconstriction were still lacking. Thus, we investigated the effects of IMiDs on smooth muscle contractility in human detrusor tissues, and porcine renal

interlobar and coronary arteries, and on proliferation, viability, apoptosis and cell death, and actin organization of primary HBdSMC.

The susceptibility of cholinergic bladder detrusor smooth muscle contractions to IMiDs differed with the cholinergic agonist and IMiD used. We observed inhibition ranging around one-third for either IMiD and cholinergic agonist in detrusor tissues, and inhibition of around 50 % in coronary arteries. Only with thalidomide, we observed no change in carbachol-induced coronary artery contraction. While detrusor smooth muscle mainly contains M2 and M3 subtypes of muscarinic receptors at a ratio of 3:1, M2 is also the predominant subtype in coronary arteries [32,40]. M3 is coupled to Gq and mediates contraction of bladder smooth muscle, whereas M2 is presumably coupled to Gi and does possibly not mediate contraction [32,40,41]. Methacholine binds in an unspecific manner to all five muscarinic receptors (M1–5), whereas carbachol does not bind to M2 receptors [32]. However, and to what extent binding of methacholine to the M2 receptor may have had an effect i.e., by increasing its affinity to M2 in the presence of thalidomide or its derivatives, or by altering the conformational state, remains purely speculative at this stage. As inhibitions of non-cholinergic contractions in detrusor tissues remained incomplete, it may be concluded that this phenomenon is not limited to muscarinic receptors but may apply to various contractile receptors in detrusor smooth muscle. However, non-cholinergic contractions were inhibited by all three IMiDs: while TXA_2-mediated contractions were inhibited the strongest across all agonist-induced contractions in detrusor tissues, U46619-induced contractions were almost completely abolished by thalidomide in coronary arteries.

While orthostatic hypotension and dizziness have been reported as rare side effects with thalidomide, these reactions may be a manifestation of autonomic neuropathy [42–44]. Vasorelaxant effects on phenylephrine-induced contractions of rat tail arteries have been suggested, following incubation with thalidomide i.e., 100 μM [45]. While vascular relaxant actions were reported, both in vivo and in vitro, relaxant actions in vitro do not seem to involve α_1-adrenoceptors, caffeine-sensitive calcium stores, glibenclamide-sensitive potassium channels, protein kinase C or P38 MAP kinase. However, actions of thalidomide resembled those of the T-type calcium channel blocker NNC 55–0396 [45]. Using a wide array of contractile agonists on human prostate, bladder, and vascular tissues, our current and recent data point to previously unreported anti-contractile activity of IMiDs through unknown mechanisms. While ligand binding studies in the above-mentioned study found no evidence for α_{1A}- or α_{1B}-adrenoceptor affinity of thalidomide, and functional studies in rat aorta found no evidence for α_{1D}-adrenoceptor binding, our data suggest divergent action of thalidomide and its derivates on α_1-adrenergic contractions: previously, we could show ubiquitous inhibition of prostate smooth muscle contraction with adrenergic and non-adrenergic agonists following incubation with IMiDs [12,13]; here, we present data showing divergent effects on α_1-adrenergic contractions in the renal artery, at least following incubation with thalidomide. We observed significant and strong inhibition of adrenergic, non-adrenergic, and neurogenic renal interlobar artery vasoconstriction, by lenalidomide and pomalidomide, and partly by thalidomide. Taken together, the effects of IMiDs on smooth muscle contraction may either be due to altering a conformational state, non-competitive receptor antagonism, or by any kind of inhibition of downstream post-receptor signaling, such as via T-type calcium channels, as previously suggested [45]. However, an extrapolation of these data as to in vivo effects on peripheral vasculature was not intended and may not be derived from our observations.

To this day, the exact mechanisms of action of thalidomide and its derivatives remain unclear, as they have the potential to work through many different pathways [31,46]. One of those mechanisms of action is anti-angiogenesis, as seen in animal corneal models [47], and proposed as possible mechanism in patients suffering from recurrent gastrointestinal bleeding sue to small-intestinal angiodysplasia [19]. While thalidomide and its derivatives also inhibit cytokines and can alter adhesion molecules, these antiangiogenic properties are likely due to inhibition of basic fibroblast growth factor (bFGF) and vascular endothelial growth factor (VEGF), suggesting a class effect [16–18,37,38,46]. Like angiogenesis, detrusor hypertrophy is a growth process, which depends on a complex network of growth factors and cytokines, which are partially overlapping with factors involved in angiogenesis [48–51]. Thalidomide may play an important role in the regulation and expression of α-smooth muscle actin (α-SMA), and certain growth factors, such as VEGF and transforming growth factor β (TGF-β) [52–54]. In parallel to androgens and inflammatory mediators, such growth factors may contribute not only to prostate growth [55,56], but simultaneously trigger bladder detrusor hypertrophy [49,57], and thus, explain the association of BPO and OAB, as both processes share common pathways.

The reduction in proliferating cells was supported by cell colony formation assays, in which we observed reduced amounts of cell colonies after treatment with either IMiD. Other than with prostatic stromal cell proliferation, we observed reduced viability of HBdSMC in a concentration- and time-dependent manner, following incubation with IMiDs. While this reduction in viability was paralleled by an increase in dead cells in flow cytometry, there were no pro-apoptotic effects. We report a discrepancy between cell viability assessed by CCK8, in which highest concentrations lead to reduced viability of 50 % or more after exposure of 72 hours, and the low number of dead cells from flow cytometry, amounting to around 10 % for all concentrations tested. While viability represents the sum of all cell cycle-relevant functions (i.e., of proliferation, apoptosis, cell death, and toxicity), this discrepancy may suggest that the decrease in viability was mostly due to reduced viability, while contributions of apoptosis/cell death were minor. However, while reduced viability may reflect the inhibitory effects observed in EdU assay and cell colony assays, the increase in dead cells on flow cytometry was minor and is unlikely to have had relevant impact on proliferation studies.

As correct organization and adequate polymerization of actin filaments are required for contraction of any smooth muscle type, and following the reports on vasorelaxant effects on phenylephrine-induced contractions of rat tail arteries [45], and on prostate smooth muscle contraction following incubation with IMiDs [12,13], we investigated the effect of IMiDs on the detrusor actin cytoskeleton. We could visualize actin filaments in cultured HBdSMC using phalloidin staining. IMiDs altered actin organization, quantitatively and qualitatively. Together with our recent findings in cultured human prostate stroma cells (WPMY-1), this may account for the inhibitory effects of thalidomide, lenalidomide and pomalidomide on prostatic, vascular and detrusor smooth muscle contraction seen in organ baths at a wide range of agonists [12,13]. As we observed varying inhibition of smooth muscle contraction on different tissue types, this may not account for the effects observed in organ bath. While solid tissues in organ baths are exposed to IMiDs for an incubation period of 45 minutes, HBdSM cells were cultured and incubated for 24 hours. Thus, the effects observed in actin visualization may not necessarily account for the inhibitory effects in organ baths. However, our data suggest vasoregulatory functions and antiproliferative properties, which may continue to expand the value of the IMiD drug class across different indications [19].

As a limitation of our study, HBdSM cells may not necessarily retain their contractile phenotype in cell culture. In parallel, expression of ion changes critical for smooth muscle excitation-contraction coupling may also be altered. Thus, cultured smooth muscle cells are considered more as a synthetic type rather than contractile type, which may differ from the situation in vivo. Depending on hypotheses tested and experimental objectives, cultured cells can still provide useful insights, as is the case in this study. Furthermore, we examined effects of pomalidomide, lenalidomide, and thalidomide on smooth muscle and vasoregulatory functions ex vivo, and proliferation of HBdSM cells in vitro at similar or higher concentrations relative to the therapeutic doses used in humans [58,59]. While appropriate scaling algorithms for in vitro studies are up for debate [60], our data are in line with current literature, exploring in

vitro efficacy of thalidomide at 100–400 μM [14,45], which is in contrast to the estimated clinically achievable plasma concentration (C_{max}) of around 3 μg/l (10 μM) [59]. For lenalidomide a different study showed that lenalidomide-triggered effects were sparse (less than 10 % compared to the negative control) at concentrations of up to 10 μM [61], which was also markedly higher than clinically achievable plasma concentrations of around 568 ng/ml (2.2 μM) [62]. That same discrepancy becomes obvious for pomalidomide in which studies explore in vitro efficacy for inducing the proliferation of T cells at 1 μM [63], while the estimated plasma concentration is around 64 ng/ml (0.23 μM) [64]. However, authors of a different study, using mice, provide an estimated plasma concentration of around 10 μM for pomalidomide [65]. While IMiDs are administered in vivo over a longer period i.e., months up to years, we have exposed tissue strips in organ baths for only 30 min incubation time, following our previously established protocols. Thus, mirroring the effects of C_{max} given for IMiDs in healthy volunteers after once oral application, may not correspond to the concentrations we used and may differ from achievable in vivo concentrations. Taken together, the concentrations used in our study correspond to the current body of literature for in vitro application of IMiDs, including our own recent data [12,13]. While our results give novel insights into previously suspected contractile functions of smooth muscle tissues [45], results may not be extrapolated to in vivo effects, without acknowledging the above-mentioned limitations. Thus, future clinical trials need to consider possible effects on smooth muscle contractility in vivo, which may offer further insight into the mechanisms of actions.

Taken together, thalidomide and its derivatives lenalidomide and pomalidomide could each target both HBdSMC proliferation and smooth muscle contraction at the same time. As both processes are crucial factors of etiology and pathophysiology of male LUTS, the optimal treatment strategy warrants addressing both at once, preferably using a single potent compound for maximum efficacy. With manageable side effects at lower dosages, all three glutamic acid derivatives could be promising candidates for in vivo application in patients with LUTS. IMiDs are orally available drugs and may show efficacy like current mono- and combination therapies by introducing inhibitory effects on prostatic and detrusor smooth muscle contraction while simultaneously reducing prostate growth and detrusor hypertrophy, without adding new side effects [66]. To the best of our knowledge, our findings are novel and promising, considering that addressing urodynamic effects in clinical trials in vivo remains mandatory for any new compound drug.

5. Conclusion

Thalidomide and its derivatives lenalidomide and pomalidomide exhibit regulatory functions in various smooth muscle-rich tissues, while impairing smooth muscle contraction and simultaneously inhibiting cell proliferation in the lower urinary tract. Future demand for new LUTS medications is high, and highest efficacy in vivo can be expected from compounds targeting prostatic and bladder detrusor smooth muscle contraction while simultaneously reducing prostate growth and detrusor hypertrophy. IMiDs facilitate cytoskeletal modulation and inhibit human detrusor smooth muscle cell growth and smooth muscle contraction. Taken together, this points to a novel drug class effect for IMiDs, in which the molecular mechanisms of action of thalidomide and its derivatives merit further consideration for the application in LUTS.

Ethics approval

Our research was carried out in accordance with the Declaration of Helsinki of the World Medical Association and has been approved by the ethics committee of Ludwig-Maximilians University, Munich, Germany. Informed consent was obtained from all patients. All samples and data were collected and analyzed anonymously.

Funding

This work was supported by grants from LMU Munich's Medical Faculty Förderprogramm für Forschung und Lehre (FöFoLe Reg.-Nr. 1092), Ferdinand Eisenberger-Forschungsstipendium der DGU (grant TaA1/FE-21), Munich Clinician Scientist Program (MCSP, Reg.-Nr. 047), and Deutsche Forschungsgemeinschaft (grant HE 5825/9–1). The funding sources had no part in study design, in the collection, analysis or interpretation of data, in the writing of the report, or in the decision to submit the article for publication.

CRediT authorship contribution statement

Stephan Ledderose: Resources, Investigation, Data curation. **Heiko Schulz:** Resources, Investigation, Data curation. **Anna Ciotkowska:** Visualization, Investigation, Formal analysis, Data curation. **Henrik Poth:** Investigation, Data curation. **Sheng Hu:** Investigation, Data curation. **Beata Rutz:** Visualization, Investigation, Formal analysis, Data curation. **Elfriede Nössner:** Writing – review & editing, Supervision, Resources, Funding acquisition. **Victor Vigodski:** Investigation, Data curation. **Thomas Kolben:** Writing – review & editing, Supervision. **Florian Springer:** Investigation, Data curation. **Martin Hennenberg:** Writing – review & editing, Supervision, Resources, Project administration, Funding acquisition, Formal analysis, Conceptualization. **Nikolaus Eitelberger:** Investigation, Data curation. **Christian G. Stief:** Writing – review & editing, Supervision, Funding acquisition. **Moritz Trieb:** Investigation, Data curation. **Nina Rogenhofer:** Writing – review & editing, Supervision. **Amin Wendt:** Investigation, Formal analysis, Data curation. **Alexander Tamalunas:** Writing – original draft, Visualization, Validation, Supervision, Methodology, Investigation, Funding acquisition, Formal analysis, Conceptualization.

Declaration of Competing Interest

The authors declare the following financial interests/personal relationships which may be considered as potential competing interests: Thomas Kolben holds stock of Roche AG and a relative is employed at Bayer AG. The other authors have no conflict of interest to declare.

Acknowledgements

We thank Prof. Dr. F. Klauschen (Institute of Pathology, Ludwig-Maximilians University, Munich) and his coworkers for the preservation of detrusor tissue samples. We thank the team of "Metzgerei Brehm" (Planegg, Germany) for providing us pig kidneys and hearts. We thank Dr. Maximilian Saller (Department of Orthopedics and Trauma Surgery, Musculoskeletal University Center Munich (MUM), University Hospital, LMU Munich, Germany) for support with immunofluorescence microscopy.

Appendix A. Supporting information

Supplementary data associated with this article can be found in the online version at doi:10.1016/j.biopha.2024.117066.

References

[1] J.N. Cornu, M. Gacci, C. Hashim, T.R.W. Herrmann, S. Malde, C. Netsch, M. Rieken, V. Sakalis, M. Tutolo, *Management of non-neurogenic male lower urinary tract symptoms (LUTS), incl. Benign prostatic obstruction (BPO)*. EAU Guidelines. Edn. presented at, EAU Annu. Congr. Milan. (March 2023). ISBN 978-94-92671-19-6., 2023.

[2] C. Chapple, Overview on the lower urinary tract, Handb. Exp. Pharm. 202 (2011) 1–14, https://doi.org/10.1007/978-3-642-16499-6_1.

[3] H. Lepor, Pathophysiology, epidemiology, and natural history of benign prostatic hyperplasia, Rev. Urol. 6 (Suppl 9) (2004) S3–S10.

[4] K.E. Andersson, A. Arner, Urinary bladder contraction and relaxation: physiology and pathophysiology, Physiol. Rev. 84 (3) (2004) 935–986, https://doi.org/10.1152/physrev.00038.2003.

[5] D.E. Irwin, Z.S. Kopp, B. Agatep, I. Milsom, P. Abrams, Worldwide prevalence estimates of lower urinary tract symptoms, overactive bladder, urinary incontinence and bladder outlet obstruction, BJU Int. 108 (7) (2011) 1132–1138, https://doi.org/10.1111/j.1464-410X.2010.09993.x.

[6] C. Chapple, W. Steers, P. Norton, R. Millard, G. Kralidis, K. Glavind, et al., A pooled analysis of three phase III studies to investigate the efficacy, tolerability and safety of darifenacin, a muscarinic M3 selective receptor antagonist, in the treatment of overactive bladder, BJU Int. 95 (7) (2005) 993–1001, https://doi.org/10.1111/j.1464-410X.2005.05454.x.

[7] C.C. Sexton, S.M. Notte, C. Maroulis, R.R. Dmochowski, L. Cardozo, D. Subramanian, et al., Persistence and adherence in the treatment of overactive bladder syndrome with anticholinergic therapy: a systematic review of the literature, Int J. Clin. Pr. 65 (5) (2011) 567–585, https://doi.org/10.1111/j.1742-1241.2010.02626.x.

[8] A. Wagg, C. Verdejo, U. Molander, Review of cognitive impairment with antimuscarinic agents in elderly patients with overactive bladder, Int J. Clin. Pr. 64 (9) (2010) 1279–1286, https://doi.org/10.1111/j.1742-1241.2010.02449.x.

[9] C. Chapple, Mirabegron the first beta3-adrenoceptor agonist for overactive bladder (OAB): a summary of the phase III studies, BJU Int 113 (6) (2014) 847–848, https://doi.org/10.1111/bju.12773.

[10] A. Athanasopoulos, C. Chapple, C. Fowler, C. Gratzke, S. Kaplan, C. Stief, et al., The role of antimuscarinics in the management of men with symptoms of overactive bladder associated with concomitant bladder outlet obstruction: an update, Eur. Urol. 60 (1) (2011) 94–105, https://doi.org/10.1016/j.eururo.2011.03.054.

[11] L. Cindolo, L. Pirozzi, C. Fanizza, M. Romero, A. Tubaro, R. Autorino, et al., Drug adherence and clinical outcomes for patients under pharmacological therapy for lower urinary tract symptoms related to benign prostatic hyperplasia: population-based cohort study, Eur. Urol. (2014), https://doi.org/10.1016/j.eururo.2014.11.006.

[12] A. Tamalunas, C. Sauckel, A. Ciotkowska, B. Rutz, R. Wang, R. Huang, et al., Inhibition of human prostate stromal cell growth and smooth muscle contraction by thalidomide: A novel remedy in LUTS? Prostate (2021) https://doi.org/10.1002/pros.24114.

[13] A. Tamalunas, C. Sauckel, A. Ciotkowska, B. Rutz, R. Wang, R. Huang, et al., Lenalidomide and pomalidomide inhibit growth of prostate stromal cells and human prostate smooth muscle contraction, Life Sci. 281 (2021) 119771, https://doi.org/10.1016/j.lfs.2021.119771.

[14] T. Ito, H. Ando, T. Suzuki, T. Ogura, K. Hotta, Y. Imamura, et al., Identification of a primary target of thalidomide teratogenicity, Science 327 (5971) (2010) 1345–1350, https://doi.org/10.1126/science.1177319.

[15] M.P. Cruz, Lenalidomide (Revlimid): a thalidomide analogue in combination with dexamethasone for the treatment of all patients with multiple myeloma, P T 41 (5) (2016) 308–313.

[16] T. Moehler, Clinical experience with thalidomide and lenalidomide in multiple myeloma, Curr. Cancer Drug Targets 12 (4) (2012) 372–390.

[17] A.M. Sales, H.J. de Matos, J.A. Nery, N.C. Duppre, E.P. Sampaio, E.N. Sarno, Double-blind trial of the efficacy of pentoxifylline vs thalidomide for the treatment of type II reaction in leprosy, Braz. J. Med. Biol. Res. 40 (2) (2007) 243–248.

[18] S.L. Walker, M.F. Waters, D.N. Lockwood, The role of thalidomide in the management of erythema nodosum leprosum, Lepr. Rev. 78 (3) (2007) 197–215.

[19] H. Chen, S. Wu, M. Tang, R. Zhao, Q. Zhang, Z. Dai, et al., Thalidomide for recurrent bleeding due to small-intestinal angiodysplasia, N. Engl. J. Med 389 (18) (2023) 1649–1659, https://doi.org/10.1056/NEJMoa2303706.

[20] A. Tamalunas, A. Buchner, A. Kretschmer, F. Jokisch, G. Schulz, L. Eismann, et al., Impact of routine laboratory parameters in patients undergoing radical cystectomy for urothelial carcinoma of the bladder: a long-term follow-up, Urol. Int. 104 (7-8) (2020) 551–558, https://doi.org/10.1159/000506263.

[21] A. Tamalunas, Y. Volz, B.A. Schlenker, A. Buchner, A. Kretschmer, F. Jokisch, et al., Is it safe to offer radical cystectomy to patients above 85 years of age? a long-term follow-up in a single-center institution, Urol. Int 104 (11-12) (2020) 975–981, https://doi.org/10.1159/000510137.

[22] A. Tamalunas, A. Wendt, F. Springer, A. Ciotkowska, B. Rutz, R. Wang, et al., Inhibition of human prostate and bladder smooth muscle contraction, vasoconstriction of porcine renal and coronary arteries, and growth-related functions of prostate stromal cells by presumed small molecule galphaq/11 inhibitor, YM-254890, Front Physiol. 13 (2022) 884057, https://doi.org/10.3389/fphys.2022.884057.

[23] B.R. Erdogan, I. Karaomerlioglu, Z.E. Yesilyurt, N. Ozturk, A.E. Muderrisoglu, M. C. Michel, et al., Normalization of organ bath contraction data for tissue specimen size: does one approach fit all? Naunyn Schmiede Arch. Pharm. 393 (2) (2020) 243–251, https://doi.org/10.1007/s00210-019-01727-x.

[24] T.T. Puck, P.I. Marcus, Action of x-rays on mammalian cells, J. Exp. Med 103 (5) (1956) 653–666.

[25] H. Rafehi, C. Orlowski, G.T. Georgiadis, K. Ververis, A. El-Osta, T.C. Karagiannis, Clonogenic assay: adherent cells, J. Vis. Exp. (49) (2011), https://doi.org/10.3791/2573.

[26] K. Feher, J. Kirsch, A. Radbruch, H.D. Chang, T. Kaiser, Cell population identification using fluorescence-minus-one controls with a one-class classifying algorithm, Bioinformatics 30 (23) (2014) 3372–3378, https://doi.org/10.1093/bioinformatics/btu575.

[27] Y. Liu, R. Huang, R. Wang, A. Tamalunas, R. Waidelich, C.G. Stief, et al., Isoform-independent promotion of contractility and proliferation, and suppression of survival by with no lysine/K kinases in prostate stromal cells, FASEB J. 38 (7) (2024) e23604, https://doi.org/10.1096/fj.202400362R.

[28] R. Huang, A. Tamalunas, R. Waidelich, F. Strittmatter, C.G. Stief, M. Hennenberg, Inhibition of full smooth muscle contraction in isolated human detrusor tissues by mirabegron is limited to off-target inhibition of neurogenic contractions, J. Pharm. Exp. Ther. (2022), https://doi.org/10.1124/jpet.121.001029.

[29] M.C. Michel, T.J. Murphy, H.J. Motulsky, New Author Guidelines for Displaying Data and Reporting Data Analysis and Statistical Methods in Experimental Biology, Mol. Pharm. 97 (1) (2020) 49–60, https://doi.org/10.1124/mol.119.118927.

[30] M.J. Curtis, S. Alexander, G. Cirino, J.R. Docherty, C.H. George, M.A. Giembycz, et al., Experimental design and analysis and their reporting II: updated and simplified guidance for authors and peer reviewers, Br. J. Pharm. 175 (7) (2018) 987–993, https://doi.org/10.1111/bph.14153.

[31] R. Eichner, M. Heider, V. Fernandez-Saiz, F. van Bebber, A.K. Garz, S. Lemeer, et al., Immunomodulatory drugs disrupt the cereblon-CD147-MCT1 axis to exert antitumor activity and teratogenicity, Nat. Med. 22 (7) (2016) 735–743, https://doi.org/10.1038/nm.4128.

[32] S.P. Alexander, A. Christopoulos, A.P. Davenport, E. Kelly, A. Mathie, J.A. Peters, et al., THE CONCISE GUIDE TO PHARMACOLOGY 2021/22: G protein-coupled receptors, Br. J. Pharm. 178 Suppl 1 (2021) S27–S156, https://doi.org/10.1111/bph.15538.

[33] X.F. Pei, T.H. Gupta, B. Badio, W.L. Padgett, J.W. Daly, 6beta-Acetoxynortropane: a potent muscarinic agonist with apparent selectivity toward M2-receptors, J. Med. Chem. 41 (12) (1998) 2047–2055, https://doi.org/10.1021/jm9705115.

[34] M. Hennenberg, C.G. Stief, C. Gratzke, Prostatic alpha1-adrenoceptors: new concepts of function, regulation, and intracellular signaling, Neurourol. Urodyn. 33 (7) (2014) 1074–1085, https://doi.org/10.1002/nau.22467.

[35] L.B. Lerner, K.T. McVary, M.J. Barry, B.R. Bixler, P. Dahm, A.K. Das, et al., Management of lower urinary tract symptoms attributed to benign prostatic hyperplasia: AUA GUIDELINE PART I-initial work-up and medical management, J. Urol. 206 (4) (2021) 806–817, https://doi.org/10.1097/JU.0000000000002183.

[36] C.R. Chapple, C.G. Roehrborn, A shifted paradigm for the further understanding, evaluation, and treatment of lower urinary tract symptoms in men: focus on the bladder, Eur. Urol. 49 (4) (2006) 651–658, https://doi.org/10.1016/j.eururo.2006.02.018.

[37] S. Joglekar, M. Levin, The promise of thalidomide: evolving indications, Drugs Today (Barc.) 40 (3) (2004) 197–204.

[38] R.A. Madan, F.H. Karzai, Y.M. Ning, B.A. Adesunloye, X. Huang, N. Harold, et al., Phase II trial of docetaxel, bevacizumab, lenalidomide and prednisone in patients with metastatic castration-resistant prostate cancer, BJU Int 118 (4) (2016) 590–597, https://doi.org/10.1111/bju.13412.

[39] J.B. Zeldis, B.A. Williams, S.D. Thomas, M.E. Elsayed, S.T.E.P.S.: a comprehensive program for controlling and monitoring access to thalidomide, Clin. Ther. 21 (2) (1999) 319–330, https://doi.org/10.1016/s0149-2918(00)88289-2.

[40] K.E. Andersson, Muscarinic acetylcholine receptors in the urinary tract, Handb. Exp. Pharm. 202 (2011) 319–344, https://doi.org/10.1007/978-3-642-16499-6_16.

[41] A. Tamalunas, A. Wendt, F. Springer, A. Ciotkowska, B. Rutz, R. Wang, et al., Inhibition of human prostate and bladder smooth muscle contraction, vasoconstriction of porcine renal and coronary arteries, and growth-related functions of prostate stromal cells by presumed small molecule Gαq/11 inhibitor, YM-254890, Front Physiol. 13 (2022), https://doi.org/10.3389/fphys.2022.884057.

[42] I.M. Ghobrial, S.V. Rajkumar, Management of thalidomide toxicity, J. Support Oncol. 1 (3) (2003) 194–205.

[43] S. Kumar, T.E. Witzig, S.V. Rajkumar, Thalidomide as an anti-cancer agent, J. Cell Mol. Med. 6 (2) (2002) 160–174, https://doi.org/10.1111/j.1582-4934.2002.tb00184.x.

[44] S.V. Rajkumar, Thalidomide in the treatment of multiple myeloma, Expert Rev. Anticancer Ther. 1 (1) (2001) 20–28, https://doi.org/10.1586/14737140.1.1.20.

[45] S.W. Seto, S. Bexis, P.A. McCormick, J.R. Docherty, Actions of thalidomide in producing vascular relaxations, Eur. J. Pharm. 644 (1-3) (2010) 113–119, https://doi.org/10.1016/j.ejphar.2010.06.035.

[46] G.D. Leonard, W.L. Dahut, J.L. Gulley, P.M. Arlen, W.D. Figg, Docetaxel and thalidomide as a treatment option for androgen- independent, nonmetastatic prostate cancer, Rev. Urol. 5 (Suppl 3) (2003) S65–S70.

[47] Y.K. Lee, S.K. Chung, The inhibitory effect of thalidomide analogue on corneal neovascularization in rabbits, Cornea 32 (8) (2013) 1142–1148, https://doi.org/10.1097/ICO.0b013e318292a79d.

[48] R. Buttyan, M.W. Chen, R.M. Levin, Animal models of bladder outlet obstruction and molecular insights into the basis for the development of bladder dysfunction, Eur. Urol. 32 (Suppl 1) (1997) 32–39.

[49] P.S. Howard, U. Kucich, D.E. Coplen, Y. He, Transforming growth factor-beta1-induced hypertrophy and matrix expression in human bladder smooth muscle cells, Urology 66 (6) (2005) 1349–1353, https://doi.org/10.1016/j.urology.2005.06.124.

[50] Y. Gao, P. Liu, F. He, X. Yang, R. Wu, W. Chen, et al., Fibroblast growth factor 2 promotes bladder hypertrophy caused by partial bladder outlet obstruction, Front Cell Dev. Biol. 9 (2021) 630228, https://doi.org/10.3389/fcell.2021.630228.

[51] M. Okada-Ban, J.P. Thiery, J. Jouanneau, Fibroblast growth factor-2, Int J. Biochem Cell Biol. 32 (3) (2000) 263–267, https://doi.org/10.1016/s1357-2725(99)00133-8.

[52] H. Arai, A. Furusu, T. Nishino, Y. Obata, Y. Nakazawa, M. Nakazawa, et al., Thalidomide prevents the progression of peritoneal fibrosis in mice, Acta Histochem Cytochem 44 (2) (2011) 51–60, https://doi.org/10.1267/ahc.10030.

[53] P. Lv, Q. Meng, J. Liu, C. Wang, Thalidomide accelerates the degradation of extracellular matrix in rat hepatic cirrhosis via down-regulation of transforming growth factor-beta1. Yonsei Med. J. 56 (6) (2015) 1572–1581, https://doi.org/10.3349/ymj.2015.56.6.1572.
[54] X. Liu, L. Qian, H. Nan, M. Cui, X. Hao, Y. Du, Function of the transforming growth factor-beta1/c-Jun N-terminal kinase signaling pathway in the action of thalidomide on a rat model of pulmonary fibrosis. Exp. Ther. Med. 7 (3) (2014) 669–674, https://doi.org/10.3892/etm.2013.1457.
[55] C. De Nunzio, F. Presicce, A. Tubaro, Inflammatory mediators in the development and progression of benign prostatic hyperplasia, Nat. Rev. Urol. 13 (10) (2016) 613–626, https://doi.org/10.1038/nrurol.2016.168.
[56] C.K. Ho, F.K. Habib, Estrogen and androgen signaling in the pathogenesis of BPH, Nat. Rev. Urol. 8 (1) (2011) 29–41, https://doi.org/10.1038/nrurol.2010.207.
[57] L.Y. Qiao, C. Xia, S. Shen, S.H. Lee, P.H. Ratz, M.O. Fraser, et al., Urinary bladder organ hypertrophy is partially regulated by Akt1-mediated protein synthesis pathway, Life Sci. 201 (2018) 63–71, https://doi.org/10.1016/j.lfs.2018.03.041.
[58] M.E. Franks, G.R. Macpherson, W.D. Figg, Thalidomide, Lancet 363 (9423) (2004) 1802–1811, https://doi.org/10.1016/S0140-6736(04)16308-3.
[59] A. Gaudy, R. Hwang, M. Palmisano, N. Chen, Population pharmacokinetic model to assess the impact of disease state on thalidomide pharmacokinetics, J. Clin. Pharm. 60 (1) (2020) 67–74, https://doi.org/10.1002/jcph.1506.
[60] J.G. Hengstler, A.K. Sjogren, D. Zink, J.J. Hornberg, In vitro prediction of organ toxicity: the challenges of scaling and secondary mechanisms of toxicity, Arch. Toxicol. 94 (2) (2020) 353–356, https://doi.org/10.1007/s00204-020-02669-7.
[61] M. Schmidt-Hieber, R. Dabrowski, A. Weimann, B. Aicher, P. Lohneis, A. Busse, et al., In vitro cytotoxicity of the novel antimyeloma agents perifosine, bortezomib and lenalidomide against different cell lines, Invest N. Drugs 30 (2) (2012) 480–489, https://doi.org/10.1007/s10637-010-9576-2.
[62] N. Chen, H. Lau, L. Kong, G. Kumar, J.B. Zeldis, R. Knight, et al., Pharmacokinetics of lenalidomide in subjects with various degrees of renal impairment and in subjects on hemodialysis, J. Clin. Pharm. 47 (12) (2007) 1466–1475, https://doi.org/10.1177/0091270007309563.
[63] G. Gorgun, E. Calabrese, E. Soydan, T. Hideshima, G. Perrone, M. Bandi, et al., Immunomodulatory effects of lenalidomide and pomalidomide on interaction of tumor and bone marrow accessory cells in multiple myeloma, Blood 116 (17) (2010) 3227–3237, https://doi.org/10.1182/blood-2010-04-279893.
[64] Z. Liu, Z. Xu, Z. Gao, Q. Ren, T. Chang, J. Xue, et al., Pharmacokinetics and bioequivalence of two pomalidomide capsules in healthy chinese subjects under fasting and fed conditions, Invest N. Drugs 41 (1) (2023) 60–69, https://doi.org/10.1007/s10637-022-01320-9.
[65] M. Shimizu, H. Suemizu, M. Mitsui, N. Shibata, F.P. Guengerich, H. Yamazaki, Metabolic profiles of pomalidomide in human plasma simulated with pharmacokinetic data in control and humanized-liver mice, Xenobiotica 47 (10) (2017) 844–848, https://doi.org/10.1080/00498254.2016.1247218.
[66] E. Fernandez-Martinez, H. Ponce-Monter, L.E. Soria-Jasso, M.I. Ortiz, J.A. Arias-Montano, G. Barragan-Ramirez, et al., Inhibition of uterine contractility by thalidomide analogs via phosphodiesterase-4 inhibition and calcium entry blockade, Molecules 21 (10) (2016), https://doi.org/10.3390/molecules21101332.